

Article

# Density, Viscosity, and Excess Properties of MDEA + H<sub>2</sub>O, DMEA + H<sub>2</sub>O, and DEEA + H<sub>2</sub>O Mixtures

Sumudu S. Karunaratne , Dag A. Eimer and Lars E. Øi \*

Faculty of Technology, Natural Sciences and Maritime Studies, University of South-Eastern Norway, Kjølnes Ring 56, 3901 Porsgrunn, Norway; sumudu.karunaratne@usn.no (S.S.K.); Dag.A.Eimer@usn.no (D.A.E.)

\* Correspondence: lars.oi@usn.no; Tel.: +47-35-575-141

Received: 16 March 2020; Accepted: 27 April 2020; Published: 3 May 2020



**Abstract:** This study presents measured density and viscosity of N-methyldiethanolamine (MDEA) + H<sub>2</sub>O, Dimethylethanolamine (DMEA) + H<sub>2</sub>O, and Diethylethanolamine (DEEA) + H<sub>2</sub>O mixtures. The density was measured at amine mass fraction  $w_1$  from 0.3 to 1 for the temperature range 293.15–353.15 K. The excess molar volumes  $V^E$  were determined from density data. Redlich–Kister type polynomials were proposed to fit  $V^E$  and density deviation  $\ln(\rho_\gamma)$  to represent measured densities. The viscosity was measured at amine mass fraction  $w_1$  from 0.3 to 1 for the temperature range 293.15–363.15 K. The viscosity deviation  $\eta^E$  and excess free energy of activation for viscous flow  $\Delta G^{E*}$  were determined from measured viscosities and examined for intermolecular interactions among mixture molecules. Correlations were proposed to fit viscosity data with acceptable accuracies. The McAllister’s three-body model was adopted to fit kinematic viscosities determined from density and dynamic viscosity data. The results showed the importance of examining intermolecular interactions that are discussed in McAllister’s four-body model to improve the accuracies of data fits.

**Keywords:** density; viscosity; MDEA; DMEA; DEEA; McAllister

## 1. Introduction

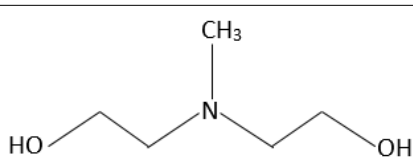
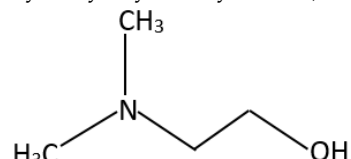
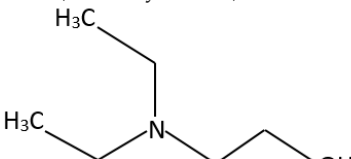
Amine-based post-combustion CO<sub>2</sub> capture (PCC) is a widely discussed emission control approach in which CO<sub>2</sub> in flue gas is captured through chemical absorption. The technology has proven the capability of over 90% of CO<sub>2</sub> removal efficiency, making amine-based PCC a reliable and economical technology [1,2]. Primary amines are highly reactive compared to secondary and tertiary amines and monoethanol amine (MEA) is the most basic of the amines in acid gas treating. The PCC with MEA is regarded as the benchmark process to compare and evaluate performance of processes with different amines for the CO<sub>2</sub> capture performance, energy utilization, and amine degradation. Tertiary amines exhibit a low absorption rate; nevertheless, fast desorption rate and high absorption capacity compared to primary amines like MEA are advantages. The reaction between CO<sub>2</sub> and MEA forms stable carbamate that limits a theoretical absorption capacity at 0.5 mol CO<sub>2</sub>/mol amine [3].

Tertiary aqueous amines like N-methyldiethanolamine (MDEA), Dimethylethanolamine (DMEA), and Diethylethanolamine (DEEA) have been studied for performance in CO<sub>2</sub> removal [4–7]. The low reaction heat of tertiary amines with CO<sub>2</sub> reduce the energy penalty due to the CO<sub>2</sub> stripping, which make the technology more feasible to use [6]. Tertiary amines do not generate carbamate during the reaction with CO<sub>2</sub>, and bicarbonate is formed as the only CO<sub>2</sub> carrying specie. This leads to increase the theoretical CO<sub>2</sub> absorption capacity up to 1 mol CO<sub>2</sub>/mol amine [3]. The characteristics shown by DMEA and DEEA in CO<sub>2</sub> absorption identify them as alternative solvents for the CO<sub>2</sub> capture processes [6,8].

Physical properties of amine solvents are useful in various aspects in process design, equipment sizing, mathematical modeling, and simulations. Density data are useful to evaluate physical solubility

of CO<sub>2</sub> in solvent, mass transfer, and solvent kinetics. Viscosity data are important to estimate diffusivity using a modified Stoke–Einstein equation [9] that is required perform calculation of mass transfer and kinetics properties [10]. Further, such data are required to build thermodynamic models and to determine model parameters [11,12]. This study provides measured density and viscosity data of aqueous MDEA, DMEA, and DEEA mixtures at different concentrations and temperatures. Table 1 provides the molecular structures and IUPAC names of pure tertiary amines. Due to improved corrosion resistant materials, the trend is to discover more concentrated amine solutions. The excess properties evaluated from measured data were compared by discussing the molecular structure and intermolecular interactions of the different tertiary amines. Density and viscosity correlations were fitted to the measured data, and accuracy of the data fit were analyzed through average absolute relative deviation (AARD %) and absolute maximum deviation (AMD).

**Table 1.** Molecular structures and IUPAC names of N-methyldiethanolamine (MDEA), Dimethylethanolamine (DMEA), and Diethylethanolamine (DEEA).

Solvent with Common Name	Molecular Structure with IUPAC Name
N-methyldiethanolamine (MDEA)	 2-(2-Hydroxyethyl-methyl-amino)ethanol
Dimethylethanolamine (DMEA)	 2-(Dimethylamino)ethanol
Diethylethanolamine (DEEA)	 2-(Diethylamino)ethanol

## 2. Materials and Methods

### 2.1. Sample Preparation

A description of the materials used in this work is listed in Table 2. A series of aqueous amine mixtures were prepared by mixing amines and water with different mass fractions. The deionized water (resistivity: 18.2 MΩ·cm) was degassed using a rotary evaporator (R-210, Buchi, Flawil, Switzerland) and used for the sample preparations. For the weight measurements, an electronic balance model—XS-403S from Mettler Toledo (Greifensee, Switzerland)—with a resolution of 1 mg was used to make a sample with 150 mL at each amine concentration.

### 2.2. Density Measurements

The density measurements of aqueous amine mixtures were performed using a DMA 4500 density meter from Anton Paar (Graz, Austria) operating at atmospheric pressure. The DMA 4500 is an oscillating U-tube density meter with an accuracy of ±0.05 kg·m<sup>3</sup>. The calibration of density meter was carried out using air and H<sub>2</sub>O at 293.15 K and a density check was performed with H<sub>2</sub>O at 293.15 K frequently to observe the validity of previous calibration. Additionally, the density of a density

reference standard S3S from Paragon Scientific Ltd. (Prenton, United Kingdom) was measured and was compared with reference values to examine any possible deviations. A sample with approximately 5 mL was introduced to the borosilicate glass U-tube (~0.7 mL) using a syringe and allowed to reach the desired temperature before the density was measured. The cell was cleaned with water, followed by ethanol, and dried with air before the next density measurement. A new sample was fed into the cell during the experiments at each different temperature levels. Final density was reported as an average of three replicates.

**Table 2.** Material description. <sup>a</sup>

Chemical Name	CAS No	Source	Purity <sup>a</sup>	Purification
MDEA	105-59-9	Merck KGaA	≥98.0	no
DEEA	100-37-8	Sigma-Aldrich	≥99.5	no
DMEA	108-01-0	Alfa Aesar	≥99.0	no

<sup>a</sup> As mentioned by the supplier.

### 2.3. Viscosity Measurements

A double-gap pressure cell XL in Physica MCR 101 rheometer from Anton Paar (Graz, Austria) was used to perform dynamic viscosity measurements in aqueous amine mixtures. The solution temperature (>303.15 K) was controlled by an internal temperature controlling system with standard temperature uncertainty 0.03 K. For the temperatures below 303.15 K, an external Anton Paar Viscotherm VT2 cooling system with standard temperature uncertainty 0.02 K was used to acquire precise temperature control [13]. In the experiments, a liquid sample with a volume of 7 mL was transferred into the pressure cell using a syringe. An adequate time was given to the sample to reach the desired temperature before taking the viscosity measurements. The experiments were repeated for three times and the final viscosity was reported as the average of 120 different readings at each temperature levels. An air check and motor adjustment were carried out prior to the experiments as suggested by Anton Paar to examine the performance of the bearing in the rotating parts. A generally used viscosity reference standard S3S from Paragon Scientific Ltd. was used to calibrate the measuring system at different temperatures. The possible viscosity deviations were recorded by comparing measured viscosity of standard oil with reference values at corresponding temperatures provided by the supplier, and corrections for the measured viscosity were made accordingly. For the temperature levels not defined by the supplier, viscosity deviations were found by interpolation. Table S1 in the supplementary material provides the information of viscosity deviations at different temperatures.

### 2.4. Measurement Uncertainty

Following uncertainty sources of material purity  $u(p_u)$ , temperature measurement  $u(T)$ , weight measurement  $u(w)$ , calibration  $u(c)$ , and repeatability  $u(rep)$  were considered to evaluate combined standard uncertainty of density and viscosity measurements of aqueous amine mixtures.

The specified standard uncertainties for the uncertainty of density measurement were  $u(p_u) = 0.006$ ,  $u(p_u) = 0.006$ ,  $u(T) = 0.012$  K,  $u(w) = 2 \times 10^{-4}$  kg,  $u(c) = 0.01$  kg·m<sup>-3</sup>, and  $u(rep) = 0.13$  kg·m<sup>-3</sup>. The maximum gradient of density against temperature,  $\partial\rho/\partial T$ , was found to be 1.2 kg·m<sup>-3</sup>·K<sup>-1</sup>, and the corresponding uncertainty in  $\rho$ ,  $(\partial\rho/\partial T) \cdot u(T)$ , was determined to be 0.02 kg·m<sup>-3</sup>. The combined standard uncertainty for the density measurement was calculated as described in the Guide to the Expression of Uncertainty in Measurement [14,15] by considering all mentioned uncertainty sources to be  $u(\rho) = 5.9$  kg·m<sup>-3</sup>. Then, the combined expanded uncertainty of the density measurement  $U(\rho)$  was found to be 11.8 kg·m<sup>-3</sup> (level of confidence = 0.95).

For the uncertainty of viscosity measurement, specified standard uncertainties for the uncertainty sources were  $u(p_u) = 0.006$ ,  $u(T) = 0.012$  K,  $u(w) = 2 \times 10^{-4}$  kg,  $u(c) = 0.065$  mPa·s, and  $u(rep) = 0.008$  mPa·s. Then the combined standard uncertainty for the viscosity measurement was calculated to

be  $u(\eta) = 0.07$  mPa·s. The combined expanded uncertainty of the viscosity measurement  $U(\eta)$  was found to be 0.14 mPa·s (level of confidence = 0.95).

### 3. Results and Discussion

#### 3.1. Density and Excess Molar Volume of the Binary Mixtures

The measured densities of pure MDEA, DMEA, and DEEA in the temperature range from 293.15 K to 353.15 K under atmospheric pressure are listed in Table 3. A comparison of measured densities of pure amines in this study with available literature data indicates that the instrument was calibrated properly prior to all experiments. The density of the aqueous amine mixtures was measured in the temperature range from 293.15 K to 343.15 K under atmospheric pressure. In the Appendix, the measured densities are presented in Tables A1–A3 under different mass fractions, mole fractions, and temperatures.

Table 3. Measured density ( $\rho/\text{kg}\cdot\text{m}^{-3}$ ) of pure amines MDEA, DMEA, and DEEA.

T/K	MDEA		DMEA		DEEA	
	This Work	Literature	This Work	Literature	This Work	Literature
293.15	1040.6		887.9	887.5 <sup>d</sup> 883.3 <sup>a</sup>	884.3	884.2 <sup>d</sup> 879.5 <sup>a</sup>
298.15	1036.8	1036.8 <sup>a</sup> , 1035.9 <sup>b</sup>	883.7	882.6 <sup>c</sup> 883.1 <sup>d</sup>	879.7	879.5 <sup>d</sup> 879.3 <sup>e</sup>
303.15	1033.1	1032.0 <sup>b</sup>	879.4	878.4 <sup>c</sup> 878.9 <sup>d</sup>	875.1	874.8 <sup>d</sup> 874.6 <sup>e</sup>
308.15	1029.3	1029.0 <sup>a</sup>	875.1	875.5 <sup>a</sup>	870.4	871.4 <sup>a</sup>
313.15	1025.5	1024.5 <sup>b</sup>	870.8	869.9 <sup>c</sup> 870.3 <sup>d</sup>	865.8	865.6 <sup>d</sup> 865.0 <sup>e</sup>
318.15	1021.7	1022.6 <sup>a</sup>	866.4	867.3 <sup>a</sup>	861.1	861.8 <sup>a</sup>
323.15	1017.9	1016.7 <sup>b</sup>	862.0		856.3	
328.15	1014.0		857.6		851.6	
333.15	1010.2	1009.0 <sup>b</sup>	853.1	851.9 <sup>c</sup>	846.8	846.5 <sup>e</sup>
338.15	1006.3		848.6		841.9	
343.15	1002.4	1001.2 <sup>b</sup>	843.8		837.1	
348.15	998.5		839.6		832.3	
353.15	994.6	993.7 <sup>b</sup>	834.7	833.8 <sup>c</sup>	827.4	827.2 <sup>e</sup>

Literature references: <sup>a</sup> Hawrylak et al. [16], <sup>b</sup> Maham et al. [17], <sup>c</sup> Maham et al. [18], <sup>d</sup> Zhang et al. [19], <sup>e</sup> Lebrette et al. [20].

Density of pure and aqueous amine mixtures decreases with increasing temperature. For the MDEA + H<sub>2</sub>O mixtures, the density starts to increase with MDEA concentration from  $x_1 = 0$  and reach a maximum value and then decreases. A shift of maximum from  $x_1 = 0.3$  at 293.15 K to  $x_1 = 0.28$  at 353.15 K was observed due to the influence from temperature. The density of DMEA + H<sub>2</sub>O and DEEA + H<sub>2</sub>O mixtures continues to decrease from  $x_1 = 0$ , and a minimum was observed at  $x_1 = 1$ . A comparison of measured density of aqueous mixtures with literature from authors Concepcion et al. [21] and Hawrylak et al. [16] is included in the supplementary materials. The comparison showed a good agreement between measured densities with available density data in the literature.

The excess molar volume  $V^E$  of a binary mixture is given by Equations (1) and (2) and is a property that can be used to fit density data of a binary mixture. The sign of  $V^E$  carries information of intermolecular interactions and molecular structure of the molecules in a mixture. The excess molar volume  $V^E$  becomes negative when the intermolecular interaction between unlike molecules are stronger than that in like molecules [22,23]. Further,  $V^E$  is negative when the molecules are efficiently packed in the solution [24]. For the mixtures having weak intermolecular interactions such as dispersion forces have positive deviation for  $V^E$  [25].

$$V^E = V - (x_1 V_1^0 + x_2 V_2^0) \quad (1)$$

$$V^E = \left[ \frac{x_1 M_1 + x_2 M_2}{\rho} \right] - \frac{x_1 M_1}{\rho_1} - \frac{x_2 M_2}{\rho_2} \quad (2)$$

The calculated  $V^E$  for MDEA + H<sub>2</sub>O, DMEA + H<sub>2</sub>O, and DEEA + H<sub>2</sub>O are shown in Tables A1–A3, respectively. The density of pure H<sub>2</sub>O was taken from the reference [26]. A negative deviation for  $V^E$  was observed for the whole range of amine concentration with a minimum in H<sub>2</sub>O-rich region at  $x_1$  of 0.36, 0.38, and 0.38 for MDEA, DMEA, and DEEA, respectively. This indicates the existence of strong intermolecular interactions like H-bonds among unlike molecules and efficient packing of molecules in the mixtures. Figure 1a,b compares the variation of  $V^E$  between three different mixtures at 293.15 K and 353.15 K.

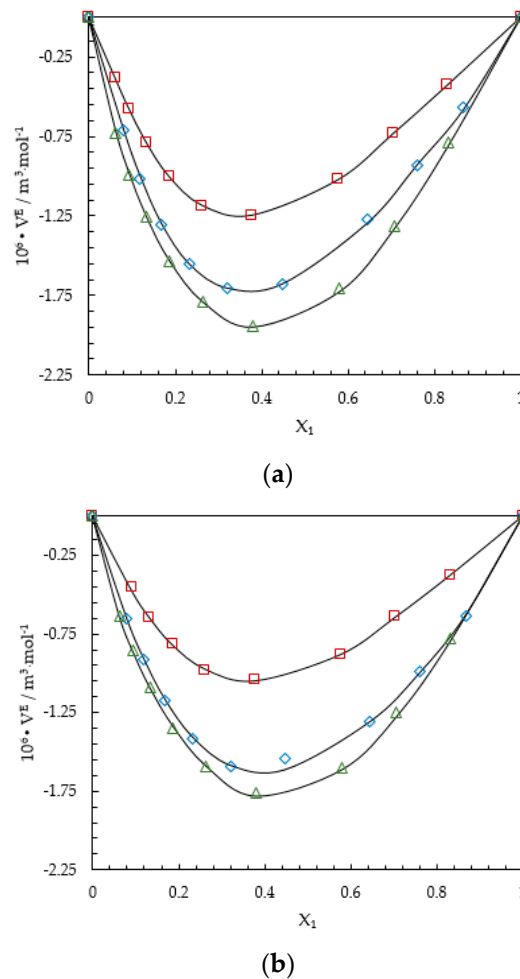


**Figure 1.** (a) Excess molar volumes  $V^E$  of MDEA (1) + H<sub>2</sub>O (2), ‘□’; DMEA (1) + H<sub>2</sub>O (2), ‘◇’ and DEEA (1) + H<sub>2</sub>O (2), ‘△’ at 293.15 K, Correlation; “—”. (b) Excess molar volumes  $V^E$  of MDEA (1) + H<sub>2</sub>O (2), ‘□’; DMEA (1) + H<sub>2</sub>O (2), ‘◇’ and DEEA (1) + H<sub>2</sub>O (2), ‘△’ at 353.15 K, Correlation; “—”.

A negative  $V^E$  or a volume contraction in the systems further reveals that considered tertiary amines and H<sub>2</sub>O are completely miscible (polar organic solvent + H<sub>2</sub>O) systems [27]. The calculated  $V^E$  for MDEA + H<sub>2</sub>O mixtures showed the lowest deviation for the range of amine concentrations compared to DMEA + H<sub>2</sub>O and DEEA + H<sub>2</sub>O mixtures. The largest deviation for  $V^E$  was observed in DEEA + H<sub>2</sub>O mixtures, indicating the existence of strong intermolecular interactions and efficient molecular packing in the mixtures. Compared to  $V^E$  of MDEA, a significant deviation was reported with DMEA ( $\approx 1.4$  times) and DEEA ( $\approx 1.6$  times) at the minimum point of 293.15 K. The substitution of

one methyl (-CH<sub>3</sub>) group for one ethanol (-CH<sub>2</sub>CH<sub>2</sub>OH) group in MDEA might results an increase of intermolecular interactions especially the H-bonding between N and OH in amine and H<sub>2</sub>O or increase of packing efficiency. Two ethyl groups (-CH<sub>2</sub>CH<sub>3</sub>) in DEEA compared to two methyl (-CH<sub>3</sub>) groups in DMEA further negatively contributed to  $V^E$ . The introduction of methyl (-CH<sub>3</sub>) or ethyl (-CH<sub>2</sub>CH<sub>3</sub>) groups increases the hydrophobicity of amine [19]. As explained by Begum et al. [23], the H<sub>2</sub>O molecules restructure around the hydrophobic part of the organic solute forming a cage-like structure. Accordingly, more structured H<sub>2</sub>O molecules around the hydrophobic groups (-CH<sub>3</sub>) and (-CH<sub>2</sub>CH<sub>3</sub>) in DMEA and DEEA, respectively, might explain the reported volume contraction in the mixtures.

A Redlich–Kister [28] type polynomial as given in the Equation (3) was proposed to fit calculated  $V^E$  for all aqueous mixtures. The measured densities at low amine concentrations (< 30% mass) presented in literature for MDEA + H<sub>2</sub>O mixtures from Maham, Teng, Mather, and Hepler [17], DMEA + H<sub>2</sub>O mixtures from Maham et al. [18], and DEEA + H<sub>2</sub>O mixtures from Lebrette et al. [20] were adopted for this work to improve the accuracy of data fitting into the proposed correlation. A temperature dependency for the Redlich-Kister coefficients ( $A_i$ ) was suggested as given in Equation (4) to determine optimum values for ( $A_i$ ) at each temperature. Table 4 lists the parameters for temperature dependency of the Redlich-Kister coefficients ( $A_i$ ) for  $V^E$  of different mixtures.

$$Y^E = x_1 x_2 \sum_{i=0}^{i=n} A_i (1 - 2x_2)^i \quad (3)$$

$$A_i = \sum_{i=0}^{i=n} a_i T^i \quad (4)$$

The partial molar volume of each component  $\bar{V}_i$  is defined as shown in Equation (5)

$$\bar{V}_i = \left( \frac{\partial V}{\partial n_i} \right)_{T, P, n_j} \quad (5)$$

For a binary mixture, partial molar volume  $\bar{V}_i$  can be determined by the following equations [29]:

$$\bar{V}_1 = V^E + V_1^0 - x_2 \left( \frac{\partial V^E}{\partial x_2} \right)_{p, T} \quad (6)$$

$$\bar{V}_2 = V^E + V_2^0 + (1 - x_2) \left( \frac{\partial V^E}{\partial x_2} \right)_{p, T} \quad (7)$$

Equations (8) and (9) can be derived by differentiating Equation (3) for  $V^E$  with respect to  $x_2$  and combining it with Equations (6) and (7).

$$\bar{V}_1 = V_1^0 + x_2^2 \sum_{i=0}^{i=n} A_i (1 - 2x_2)^i + 2x_2^2 (1 - x_2) \sum_{i=0}^{i=n} A_i (i) (1 - 2x_2)^{i-1} \quad (8)$$

$$\bar{V}_2 = V_2^0 + (1 - x_2)^2 \sum_{i=0}^{i=n} A_i (1 - 2x_2)^i - 2x_2 (1 - x_2)^2 \sum_{i=0}^{i=n} A_i (i) (1 - 2x_2)^{i-1} \quad (9)$$

The partial molar volume of amines at infinite dilution in H<sub>2</sub>O  $\bar{V}_1^\infty$  can be determined by considering the scenario of  $x_2 = 1$  as given in the Equation (10) and partial molar volume of H<sub>2</sub>O at infinite dilution in amines  $\bar{V}_2^\infty$  can be found by considering the scenario of  $x_2 = 0$  as shown in Equation (11).

$$\bar{V}_1^\infty = V_1^0 + \sum_{i=0}^{i=n} A_i (-1)^i \quad (10)$$

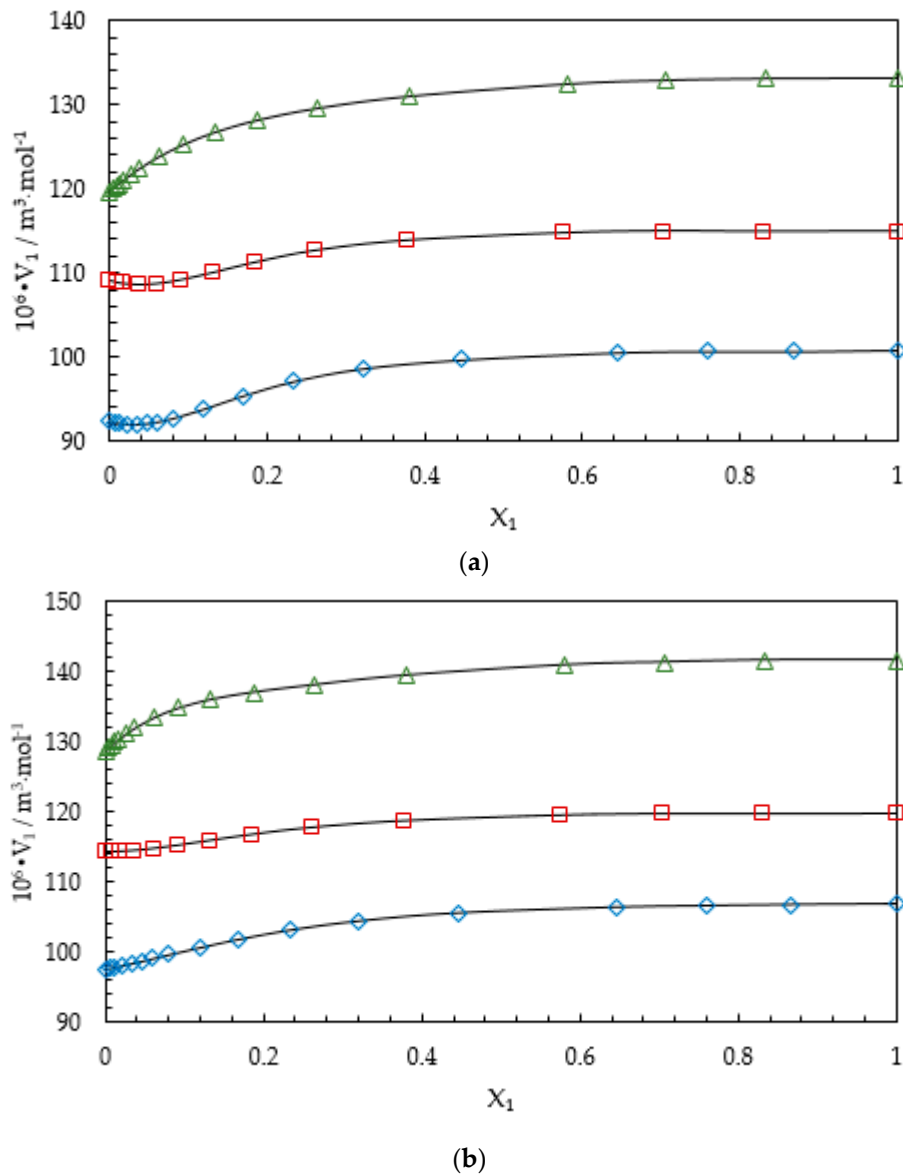
$$\bar{V}_2^\infty = V_2^0 + \sum_{i=0}^{i=n} A_i \quad (11)$$

Table A4 presents the calculated partial molar volume  $\bar{V}_1^\infty$  of amines at infinite dilution in H<sub>2</sub>O with molar volume  $V_1^0$  of pure amines. The proposed temperature dependency for the Redlich-Kister coefficients ( $A_i$ ) was able to calculate  $\bar{V}_1^\infty$  with a deviation around 1% AARD compared to literature data. The partial molar volume  $\bar{V}_1^\infty$  of amines were smaller than the corresponding molar volume  $V_1^0$  of pure amines. This can be explained for MDEA, DMEA and DEEA by the existence of (partially) ice-like structure in pure H<sub>2</sub>O [30], which is more open than a nearly close packed arrangement, enables to fit (partially) amine molecules into the open or empty spaces in liquid H<sub>2</sub>O [29]. Hepler [30] explained structure making solute and structure breaking solute based on the sign of  $(\partial^2 \bar{V}_1^\infty / \partial T^2)_P$ , in which the positive sign is associated with structure making solute, while the negative sign is associated with structure breaking solute. The study shows that for all considered tertiary amines, variation of  $\bar{V}_1^\infty$  with temperature is linear ( $R^2 > 0.999$ ) by making the first derivative of  $\bar{V}_1^\infty$  with respect to temperature a positive constant. This does not provide any information about second derivation for a positive or a negative sign. A similar observation was reported by Maham, Teng, Hepler, and Mather [29] for MDEA. Accordingly, this does not indicate that MDEA, DMEA, and DEEA in dilute aqueous mixtures can be considered as either net structure makers or net structure breakers. Figure 2a,b illustrate the composition dependence of the partial molar volume of MDEA in (MDEA + H<sub>2</sub>O), DMEA in (DMEA + H<sub>2</sub>O), and DEEA in (DEEA + H<sub>2</sub>O) at 298.15 K and 353.15 K, respectively. Figure 2a shows a minimum value for  $\bar{V}_1$  around  $x_1 = 0.04$  for MDEA and DMEA at 298.15 K and it disappears with the increase of temperature, as shown in Figure 2b.

**Table 4.** Temperature dependency of the Redlich–Kister coefficients ( $A_i$ ) for the excess molar volume ( $10^6 \cdot V^E/\text{m}^3 \cdot \text{mol}^{-1}$ ) of different aqueous amine mixtures.

Parameters	Mixtures					
	MDEA (1) + H <sub>2</sub> O (2)		DMEA (1) + H <sub>2</sub> O (2)		DEEA (1) + H <sub>2</sub> O (2)	
	$a_0$	$a_1$	$a_0$	$a_1$	$a_0$	$a_1$
$A_0$	−7.847	0.0111	−7.363	0.00313	−10.120	0.00884
$A_1$	5.378	−0.00932	6.103	−0.01065	5.082	−0.00770
$A_2$	−2.584	0.00663	−1.532	0.00017	−2.175	0.00491
$A_3$	8.187	−0.02062	18.490	−0.05285	13.530	−0.04196
$A_4$	1.599	−0.00537	−0.774	0.00274	−2.203	0.00395
$A_5$	−15.300	0.03798	−29.660	0.08247	−16.060	0.05570
AARD (%)	0.007		0.015		0.011	
AMD (kg·m <sup>3</sup> )	0.97		1.04		0.80	

The accuracy of the data fit was determined by average absolute relative deviation (AARD) and absolute maximum deviation (AMD) as given in Equations (12) and (13). A density correlation based on a Redlich-Kister type polynomial for  $V^E$  and density deviation defined as  $\ln(\rho_\gamma)$  in Equation (15) were examined to fit the measured densities of MDEA + H<sub>2</sub>O, DMEA + H<sub>2</sub>O and DEEA + H<sub>2</sub>O mixtures at different concentrations and temperatures.



**Figure 2.** (a) Partial molar volumes of MDEA in (MDEA + H<sub>2</sub>O), ‘□’; DMEA in (DMEA + H<sub>2</sub>O), ‘◇’ and DEEA in (DEEA + H<sub>2</sub>O), ‘△’ at 298.15 K. (b) Partial molar volumes of MDEA in (MDEA + H<sub>2</sub>O), ‘□’; DMEA in (DMEA + H<sub>2</sub>O), ‘◇’ and DEEA in (DEEA + H<sub>2</sub>O), ‘△’ at 353.15 K.

Average absolute relative deviation:

$$AARD (\%) = \frac{100\%}{N} \sum_{i=1}^{i=N} \left| \frac{Y_i^m - Y_i^c}{Y_i^m} \right| \tag{12}$$

Absolute maximum deviation:

$$AMD = \max |Y_i^m - Y_i^c| \tag{13}$$

For binary mixtures, the use of excess molar volume to correlate mixture density is a widely adopted approach described in Equation (14). The evaluated correlation parameters for different mixtures are listed in Table 5 with relevant AARD and AMD.



$$\rho = \frac{\sum_{i=1}^2 x_i M_i}{V^E + \sum_{i=1}^2 \frac{x_i M_i}{\rho_i}} \quad (14)$$

$$\ln(\rho) = \ln(\rho_\gamma) + \sum_{i=1}^2 x_i \rho_i \quad (15)$$

$$\ln(\rho_\gamma) = x_1 x_2 \sum_{i=0}^{i=n} A_i (1 - 2x_2)^i \quad (16)$$

**Table 5.** Temperature dependency of the Redlich–Kister coefficients ( $A_i$ ) for the density deviation  $\ln(\rho_\gamma)$  of different aqueous amine mixtures.

Parameters	Mixtures					
	MDEA (1) + H <sub>2</sub> O (2)		DMEA (1) + H <sub>2</sub> O (2)		DEEA (1) + H <sub>2</sub> O (2)	
	$a_0$	$a_1$	$a_0$	$a_1$	$a_0$	$a_1$
$A_0$	0.3054	$-6.25 \times 10^{-4}$	0.2197	$-9.27 \times 10^{-4}$	0.2491	$-11.42 \times 10^{-4}$
$A_1$	-0.4206	$8.48 \times 10^{-4}$	-0.3892	$12 \times 10^{-4}$	-0.4277	$14.91 \times 10^{-4}$
$A_2$	0.4459	$-9.12 \times 10^{-4}$	0.3690	$-10.5 \times 10^{-4}$	0.5542	$-17.69 \times 10^{-4}$
AARD (%)	0.1		0.03		0.04	
AMD (kg·m <sup>-3</sup> )	3.0		1.5		2.7	

For MDEA + H<sub>2</sub>O mixtures, a maximum deviation of measured density from the correlation was found at MDEA mole fraction  $x_1 = 0.0916$  and temperature 353.15 K. Similarly, for DMEA + H<sub>2</sub>O and DEEA + H<sub>2</sub>O mixtures, maximum deviations were reported at  $x_1 = 0.447$  and  $x_1 = 0.0618$  at temperature 353.15 K and 293.15 K, respectively. Table 5 lists the calculated parameters for the correlation based on density deviation with corresponding AARD and AMD for each binary mixture. It was observed that MDEA + H<sub>2</sub>O shows a maximum deviation of measured density from the correlation at  $x_1 = 0.5764$  at 293.15 K. For the DMEA + H<sub>2</sub>O mixtures, a maximum deviation of measured density from the correlation was found at  $x_1 = 0.1187$  at 293.15 K, while DEEA + H<sub>2</sub>O mixtures revealed a maximum deviation at  $x_1 = 0.0618$  at 293.15 K. The study showed that the correlation based on  $V^E$  for density provided higher accuracies in the data fits. However, the reported accuracies from both considered correlations are acceptable to use them in the engineering calculations.

### 3.2. Viscosity of the Binary Mixtures

A comparison of measured viscosity of pure amines in this study with available data in the literature is given in Table 6. The study shows that measured viscosities agree with literature data with around 3.5% AARD. The measured viscosities of the binary aqueous mixtures are shown in Table A5, Table A6, and Table A7. The mixture viscosity varies with the composition and temperature. For the MDEA + H<sub>2</sub>O mixtures at 293.15 K, a maximum viscosity was observed around  $x_1 = 0.7$ . The study shows that DEEA + H<sub>2</sub>O mixtures have a maximum viscosity around  $x_1 = 0.36$  at 293.15 K and the DMEA + H<sub>2</sub>O mixtures exhibit a maximum viscosity around  $x_1 = 0.38$  at 293.15 K. The measured viscosities of aqueous mixtures were compared with viscosities presented by Concepcion et al. [21], Teng et al. [31], Garcia et al. [32], and Maham et al. [33] in the supplementary materials. Figure 3 compares viscosity variations of different aqueous amine mixtures at 293.15 K.

The viscosity deviation  $\eta^E$  or the excess viscosity of the mixtures is calculated as shown in Equation (17). The viscosity of pure H<sub>2</sub>O was taken from Korson et al. [34].

$$\eta^E = \eta - \sum_{i=1}^{i=2} x_i \eta_i \quad (17)$$

According to Kauzmann and Eyring [35], the viscosity of a mixture strongly depends on the entropy of the mixture that is related to the liquid’s structure and bond enthalpy and consequently with the intermolecular interactions between components in the mixture [36]. Hence, viscosity deviation is attributed to the difference in size and shape of the component molecules and molecular interactions between unlike molecules such as H-bonds (strong interactions) and dispersion forces (weak interactions). The value of  $\eta^E$  becomes positive due to the presence of strong interactions like H-bond formation [37] and  $\eta^E$  is negative where the weak interactions (weak dipole and dispersion forces) are dominant [37,38].

**Table 6.** Measured viscosity ( $\eta$ /mPa·s) of pure amines MDEA, DMEA, and DEEA.

T/K	MDEA		DMEA		DEEA	
	This Work	Literature	This Work	Literature	This Work	Literature
293.15	100.72		3.89		4.95	
298.15	75.90	77.19 <sup>a</sup>	3.39		4.17	4.02 <sup>b</sup>
303.15	57.82		2.96		3.54	3.31 <sup>b</sup>
308.15	44.62		2.59		3.01	
313.15	34.89	34.11 <sup>a</sup>	2.28	2.24 <sup>c</sup>	2.58	2.41 <sup>b</sup>
318.15	27.67		2.01		2.24	
323.15	22.22		1.79	1.76 <sup>c</sup>	1.95	
328.15	18.10		1.60		1.71	
333.15	14.89	14.30 <sup>a</sup>	1.43	1.41 <sup>c</sup>	1.51	1.44 <sup>b</sup>
338.15	12.38		1.29		1.35	
343.15	10.38	9.85 <sup>a</sup>	1.17	1.16 <sup>c</sup>	1.21	
348.15	8.78		1.05		1.09	
353.15	7.48	7.12 <sup>a</sup>	0.96	0.96 <sup>c</sup>	0.98	0.93 <sup>b</sup>
358.15	6.43		0.87		0.90	
363.15	5.56		0.80		0.82	

Literature references: <sup>a</sup> Teng et al. [31], <sup>b</sup> Maham et al. [33], <sup>c</sup> Garcia et al. [32].

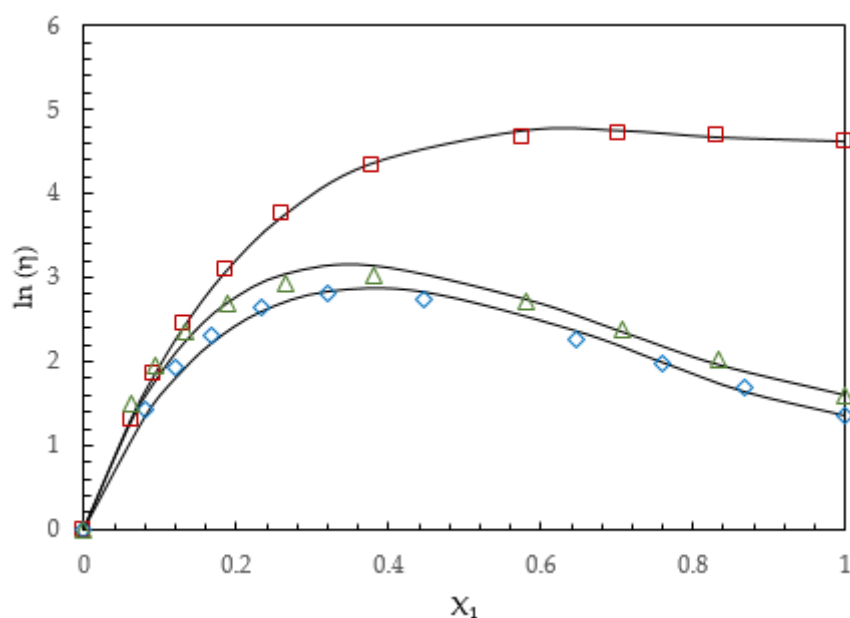


**Figure 3.** Viscosities of MDEA (1) + H<sub>2</sub>O (2), ‘□’; DMEA (1) + H<sub>2</sub>O (2), ‘◇’ and DEEA (1) + H<sub>2</sub>O (2), ‘△’ mixtures at 293.15 K, Correlation; “—”.

The semiempirical model suggested by Grunberg and Nissan [39] can be adopted to interpret the strength of the molecular interactions between components in a binary mixture [37]. The model is

consisting of one adjustable parameter  $G_{12}$  that is beneficial to correlate dynamic viscosity of binary mixtures using pure component viscosities. The model for a binary mixture is given as follows.

$$\ln(\eta) = \sum_{i=1}^{i=2} x_i \ln(\eta_i) + x_1 x_2 G_{12} \quad (18)$$

The sign of  $G_{12}$  gives similar information as  $\eta^E$  for the liquid mixtures. Accordingly,  $G_{12}$  is negative for systems in which dispersion forces are dominant and  $G_{12}$  become positive as the strength of the intermolecular interaction increases [37].

The dynamic viscosity model proposed by Eyring [40] based on the theory of absolute reaction rate provides another approach to examine the molecular interaction in a binary mixture. For a liquid mixture, the viscosity is represented according to the Eyring's model as follows:

$$\eta = \frac{hN_A}{V} \exp\left(\frac{\Delta G^*}{RT}\right) \quad (19)$$

Accordingly, excess free energy of activation for viscous flow  $\Delta G^{E*}$  is defined as follows using pure component viscosities and molar volumes.

$$\ln(\eta V) = \ln(\eta V)_{ideal} + \frac{\Delta G^{E*}}{RT} \quad (20)$$

$$\ln(\eta V) = \sum_{i=1}^{i=2} x_i \ln(\eta_i V_i^0) + \frac{\Delta G^{E*}}{RT} \quad (21)$$

Meyer et al. [41] discussed the applicability of the sign of  $\Delta G^{E*}$  as in viscosity deviation  $\eta^E$  to understand the types of intermolecular interactions. It has been reported by authors [41–44] that the positive  $\Delta G^{E*}$  indicates strong interactions like H-bond and negative  $\Delta G^{E*}$  signifies weak molecular interactions like dispersion forces. The  $\ln(\eta_\gamma)$  shown in Equation (22) is similar to the term  $x_1 x_2 G_{12}$  in the Grunberg and Nissan [39] model. Figure 4a–c illustrate the variation of  $\eta^E$ ,  $\ln(\eta_\gamma)$  and  $\Delta G^{E*}$  with amine concentration in different mixtures at 293.15 K.

$$\ln(\eta) = \ln(\eta_\gamma) + \sum_{i=1}^{i=2} x_i \ln(\eta_i) \quad (22)$$

Figure 4a shows that  $\eta^E$  was negative for low MDEA concentrations indicating the presence of weak intermolecular interactions like weak dipole and dispersion forces. As MDEA concentration increases,  $\eta^E$  becomes positive and shows a maximum in the amine-rich region, signifying the existence of strong intermolecular interactions like H-bonds among unlike molecules. The DMEA + H<sub>2</sub>O and DEEA + H<sub>2</sub>O mixtures showed positive deviation for  $\eta^E$  for the whole amine concentrations, revealing that the intermolecular interactions between those amines and H<sub>2</sub>O are stronger than interactions between like molecules. For DMEA + H<sub>2</sub>O and DEEA + H<sub>2</sub>O mixtures, the maximum  $\eta^E$  was observed in the H<sub>2</sub>O rich region. The highest positive deviation for  $\eta^E$  was reported by MDEA + H<sub>2</sub>O mixtures around  $x_1 = 0.6$ . The DMEA + H<sub>2</sub>O and DEEA + H<sub>2</sub>O mixtures reached their highest  $\eta^E$  around  $x_1 = 0.35$ . DMEA + H<sub>2</sub>O and DEEA + H<sub>2</sub>O mixtures showed a similar behavior for  $\eta^E$ , while MDEA + H<sub>2</sub>O mixtures showed deviations indicating the influence of (-OH) groups in MDEA on viscosity of aqueous mixtures. The calculated  $G_{12}$  and  $\Delta G^{E*}$  showed positive deviations for all considered aqueous amine mixtures for the whole range of amine concentrations. This shows that the considered aqueous amine mixtures are having strong intermolecular interactions among unlike molecules for the whole range of amine concentrations. The MDEA + H<sub>2</sub>O mixtures showed a highest peak around  $x_1 = 0.35$ , while DMEA + H<sub>2</sub>O and DEEA + H<sub>2</sub>O mixtures showed peaks around  $x_1 = 0.3$  and  $x_1 = 0.25$ , respectively. Figure 4c illustrates that DEEA + H<sub>2</sub>O mixtures have a higher  $\Delta G^{E*}$  in H<sub>2</sub>O rich region than MDEA +

H<sub>2</sub>O mixtures and  $\Delta G^{E*}$  of MDEA + H<sub>2</sub>O showed higher values than DMEA + H<sub>2</sub>O and DEEA + H<sub>2</sub>O for the amine rich region. However,  $\Delta G^{E*}$  does not show a large deviation among the different amine mixtures as in  $\eta^E$ . This can be assumed due to the influence of molecular packing in the mixtures on viscous flow.

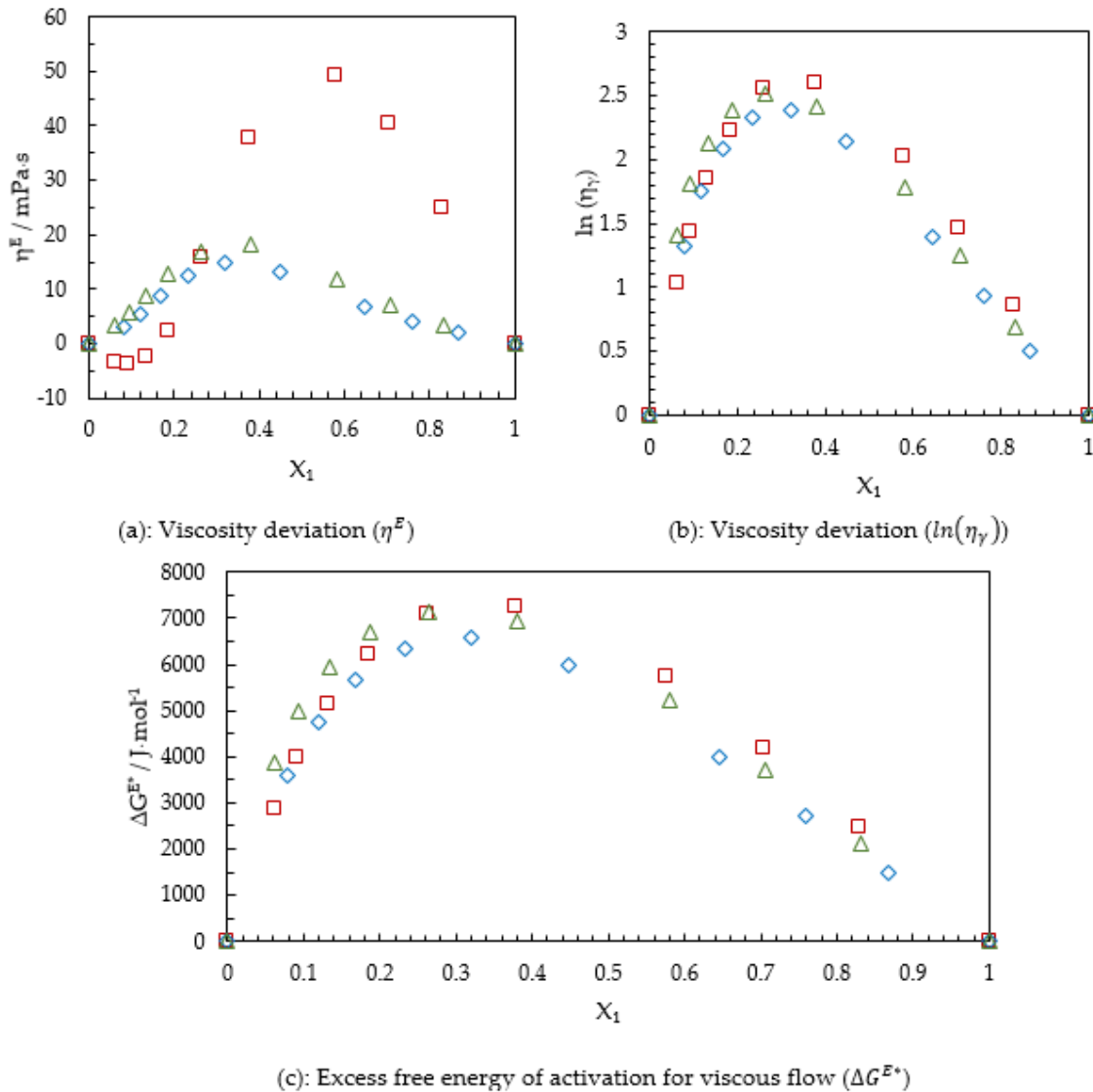


**Figure 4.** (a–c)  $\eta^E$ ,  $\ln(\eta_\gamma)$  and  $\Delta G^{E*}$  of MDEA (1) + H<sub>2</sub>O (2), ‘□’; DMEA (1) + H<sub>2</sub>O (2), ‘◇’ and DEEA (1) + H<sub>2</sub>O (2), ‘△’ mixtures at 293.15 K.

The slope of the excess free energy of activation for viscous flow  $\Delta G^{E*}$  against temperature ( $T$ ) carries the information about the excess entropy of activation for viscous flow  $\Delta S^{E*}$  as given in Equation (23). The plot of  $\Delta G^{E*}$  versus temperature ( $T$ ) was linear in the temperature range from 293.15 K to 363.15 K at a certain mole fraction for the mixtures studied.

$$\Delta S^{E*} = - \left[ \frac{\partial(\Delta G^{E*})}{\partial T} \right] \tag{23}$$

Figure 5 illustrates the excess entropy of activation for viscous flow  $\Delta S^{E*}$  for MDEA + H<sub>2</sub>O, DMEA + H<sub>2</sub>O and DEEA + H<sub>2</sub>O mixtures over the whole range of concentrations. Equation (23) was adopted to calculate  $\Delta S^{E*}$  for temperature range 293.15–363.15 K. Similar to the  $\Delta G^{E*}$  variation with the mole fraction,  $\Delta S^{E*}$  increases with the increase of mole fraction up to a maximum and then

decreases. The peaks were observed around  $x_1 = 0.38$  for MDEA + H<sub>2</sub>O and DEEA + H<sub>2</sub>O mixtures, while DMEA + H<sub>2</sub>O showed a peak around  $x_1 = 0.32$ . The  $\Delta S^{E*}$  of DEEA + H<sub>2</sub>O mixtures was higher than that of MDEA + H<sub>2</sub>O and DMEA + H<sub>2</sub>O mixtures for the whole range of amine concentration.

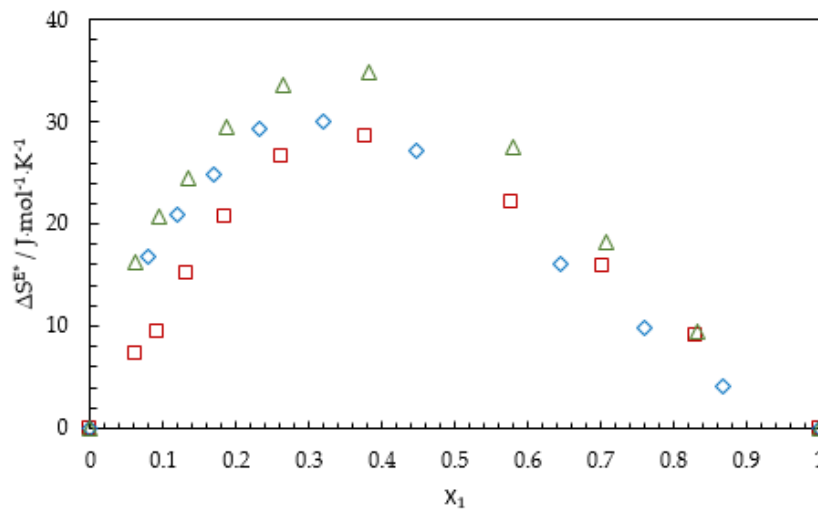


**Figure 5.** Excess entropy of activation for viscous flow ( $\Delta S^{E*}$ ) for MDEA (1) + H<sub>2</sub>O (2), ‘□’; DMEA (1) + H<sub>2</sub>O (2), ‘◇’ and DEEA (1) + H<sub>2</sub>O (2), ‘△’ mixtures as a function of mole fractions.

The measured viscosities from 293.15 K to 363.15 K of the mixtures were fitted to the empirical correlation shown in Equation (22). The Redlich–Kister model [28] is a good candidate to correlate excess properties in a binary mixtures. In order to acquire a good accuracy in data fit, a higher degree polynomial is required with a large number of fitting parameters. A simplified lower degree polynomial was suggested as given in Equation (24). Similar work have been reported by Hartono et al. [45] for the viscosity of MEA + H<sub>2</sub>O mixtures.

$$\ln(\eta_\gamma) = (A_0 + A_1T + A_2T^2 + A_3x_1 + A_4Tx_1^2 + A_5x_1^3) \cdot x_1x_2 \tag{24}$$

Table 7 lists the calculated parameters of Equation (24) for different mixtures. The correlations provide acceptable accuracies for use in engineering calculations. For MDEA + H<sub>2</sub>O mixtures, AMD shows a relatively high deviation as 6.4 mPa·s, but measured viscosity is as high as 114.261 mPa·s.

**Table 7.** Coefficients ( $A_i$ ) for the viscosity deviation  $\ln(\eta_\gamma)$  of different aqueous amine mixtures.

Parameters	Mixtures		
	MDEA (1) + H <sub>2</sub> O (2)	DMEA (1) + H <sub>2</sub> O (2)	DEEA (1) + H <sub>2</sub> O (2)
$A_0$	98.13	99.61	123.5
$A_1$	−0.4163	−0.4218	−0.528
$A_2$	$5.008 \times 10^{-4}$	$5.013 \times 10^{-4}$	$6.291 \times 10^{-4}$
$A_3$	−29.09	−33.79	−45.8
$A_4$	0.0838	0.1083	0.1498
$A_5$	−10.47	−14.69	−18.31
AARD (%)	1.7	2.7	4.7
AMD (mPa·s)	6.4	1.3	2.4

McAllister [46] developed a semiempirical model based on Eyring’s theory of absolute reaction rates to represent kinematic viscosities in a binary mixture. The McAllister [46] three-body model considered interactions among three molecules that are all in one plane.

The McAllister's three-body model:

$$\begin{aligned} \ln(v) = & x_1^3 \cdot \ln(v_1) + 3x_1^2x_2 \cdot \ln(v_{12}) + 3x_1x_2^2 \cdot \ln(v_{21}) + x_2^3 \cdot \ln(v_2) \\ & - \ln(x_1 + x_2 \cdot [M_2/M_1]) + 3x_1^2x_2 \\ & \cdot \ln([2 + M_2/M_1]/3) + 3x_1x_2^2 \cdot \ln([1 + 2M_2/M_1]/3) + x_2^3 \cdot \ln(M_2/M_1) \end{aligned} \quad (25)$$

McAllister's three-body model have two fitting parameters of  $v_{12}$  and  $v_{21}$ . For each type of  $\Delta G^*$  considered during the model development, a corresponding kinematic viscosity were assigned as shown in Equations (26)–(30). With the assumption of temperature independent enthalpies and entropies of activation for viscous flow, it provides a kinematic viscosity model with both composition and temperature as independent variables. The unknown enthalpies and entropies can be calculated by fitting kinematic viscosity data at different compositions and temperatures to the model. Our previous work based on kinematic viscosities of MEA (monoethanol amine) + H<sub>2</sub>O mixtures provided acceptable accuracies by following this method [47].

$$\Delta G^* = \Delta H^* - T\Delta S^* \quad (26)$$

$$v_1 = \frac{hN}{M_1} e^{-\Delta s_1^*/R} e^{\Delta H_1^*/RT} \quad (27)$$

$$v_{12} = \frac{hN}{M_{12}} e^{-\Delta s_{12}^*/R} e^{\Delta H_{12}^*/RT} \quad (28)$$

$$v_{21} = \frac{hN}{M_{21}} e^{-\Delta s_{21}^*/R} e^{\Delta H_{21}^*/RT} \quad (29)$$

$$v_2 = \frac{hN}{M_2} e^{-\Delta s_2^*/R} e^{\Delta H_2^*/RT} \quad (30)$$

The explained approach was adopted in this study to represent kinematic viscosities that were calculated via measured dynamic viscosities and densities. It was calculated accuracies as 23%, 17%, and 15% for MDEA + H<sub>2</sub>O, DMEA + H<sub>2</sub>O, and DEEA + H<sub>2</sub>O mixtures. These deviations are relatively high and questioning that adopted method with McAllister's three-body model is viable to use for correlating kinematic viscosities of the considered mixtures. Accordingly, kinematic viscosity data were fitted at different temperatures instead of a temperature range using Equation (25) to see improvements in the accuracies. The reported AARD using Equation (25) are 8.4 %, 9.2% and 16% for MDEA + H<sub>2</sub>O, DMEA + H<sub>2</sub>O, and DEEA + H<sub>2</sub>O mixtures. It indicates that data fitting at different temperatures improves the accuracies of viscosity representation except for the DEEA + H<sub>2</sub>O. Table 8 lists the calculated parameters of Equation (25) at different temperatures. McAllister stated the necessity of taking into account other interactions that are involving more than three molecules in a three dimensional space instead of one plane for the scenario of two types of molecules having a size (radius) difference by more than a factor of 1.5 [46]. McAllister's four-body model discusses such interactions however the fitting of kinematic viscosity data into four-body model is not discussed in this work.

**Table 8.** Calculated parameters of McAllister's three-body model.

T/K	Mixtures					
	MDEA (1) + H <sub>2</sub> O (2)		DMEA (1) + H <sub>2</sub> O (2)		DEEA (1) + H <sub>2</sub> O (2)	
	$10^6 \cdot v_{12}$	$10^6 \cdot v_{21}$	$10^6 \cdot v_{12}$	$10^6 \cdot v_{21}$	$10^6 \cdot v_{12}$	$10^6 \cdot v_{21}$
293.15	44.0582	2089.1458	3.2724	596.7573	2.7885	1646.6703
298.15	33.9711	1340.1148	2.9023	385.8739	2.3762	1001.7568
303.15	26.1935	883.1637	2.6000	255.3182	2.0452	624.2248
308.15	20.3995	597.3544	2.3060	173.9052	1.7780	402.8284
313.15	16.2081	414.6814	2.0658	121.4510	1.5613	266.5363
318.15	13.0073	296.0447	1.8692	87.3140	1.3573	184.4744

Table 8. Cont.

T/K	Mixtures					
	MDEA (1) + H <sub>2</sub> O (2)		DMEA (1) + H <sub>2</sub> O (2)		DEEA (1) + H <sub>2</sub> O (2)	
	10 <sup>6</sup> · v <sub>12</sub>	10 <sup>6</sup> · v <sub>21</sub>	10 <sup>6</sup> · v <sub>12</sub>	10 <sup>6</sup> · v <sub>21</sub>	10 <sup>6</sup> · v <sub>12</sub>	10 <sup>6</sup> · v <sub>21</sub>
323.15	10.4386	216.2663	1.6745	64.2968	1.1800	131.5663
328.15	8.5464	162.4728	1.5001	48.5945	1.0466	96.5934
333.15	7.0675	124.2767	1.3573	37.5439	0.9282	72.6396
338.15	5.8446	97.0776	1.2282	29.5331	0.8151	56.2896
343.15	4.8818	77.1314	1.1113	23.7008	0.7229	44.5010
348.15	4.2867	59.2349	1.0055	19.2115	0.6412	35.7128
353.15	3.6529	48.6431	0.9190	15.7291	0.5801	28.9483
AARD (%)	8.4		9.2		16	

#### 4. Conclusions

Densities of MDEA + H<sub>2</sub>O, DMEA + H<sub>2</sub>O, and DEEA + H<sub>2</sub>O mixtures were measured for amine mass fraction range from 0.3 to 1 and for the temperature range from 293.15 K to 353.15 K. The measured density of MDEA + H<sub>2</sub>O mixtures increases with increase of MDEA concentration until a maximum and then decreases. For the density of DMEA + H<sub>2</sub>O and DEEA + H<sub>2</sub>O mixtures, a density maximum reported at  $x_1 = 0$  and density continues to decrease with increase of amine concentration. The excess molar volumes  $V^E$  were negative for the all mixtures and temperature dependent. This indicates efficient molecular packing and existence of strong intermolecular interactions such as H-bonds among unlike molecules in the mixtures. The density correlations based on Redlich–Kister type polynomials for excess molar volume  $V^E$  and density deviation  $\ln(\rho_\gamma)$  represented measured densities with good accuracy signifying their applicability to perform engineering calculations. The proposed Redlich–Kister type polynomials with linear temperature dependency were able to calculate partial molar volume  $\bar{V}_1^\infty$  of amines at infinite dilution in H<sub>2</sub>O with acceptable accuracies compared to values reported in literature.

Viscosities of MDEA + H<sub>2</sub>O, DMEA + H<sub>2</sub>O, and DEEA + H<sub>2</sub>O mixtures were measured for amine mass fraction  $w_1$  range from 0.3 to 1 for the temperature range from 293.15 K to 363.15 K. The calculated viscosity deviation  $\eta^E$  and excess free energy of activation for viscous flow  $\Delta G^{E*}$  could be explained the intermolecular interactions among unlike molecules in the mixtures. The proposed viscosity correlations were able to represent measured data with acceptable accuracies. The McAllister's three-body model was adopted to correlate kinematic viscosities calculated from measured viscosities and densities at different concentrations and temperatures. The accuracies of the data fits into McAllister's three-body model are relatively low compared to the proposed viscosity correlations in this work and it is recommended to examine McAllister's four-body model for better data representation.

**Supplementary Materials:** The following are available online at <http://www.mdpi.com/2076-3417/10/9/3196/s1>, Figure S1: Comparison of measured density of MDEA (1) + H<sub>2</sub>O (2) mixtures with literature, Figure S2: Comparison of measured density of DMEA (1) + H<sub>2</sub>O (2) mixtures with literature, Figure S3: Comparison of measured density of DEEA (1) + H<sub>2</sub>O (2) mixtures with literature, Figure S4: Comparison of measured viscosity of MDEA (1) + H<sub>2</sub>O (2) mixtures with literature, Figure S5: Comparison of measured viscosity of DMEA (1) + H<sub>2</sub>O (2) mixtures with literature, Figure S6: Comparison of measured viscosity of DEEA (1) + H<sub>2</sub>O (2) mixtures with literature, Table S1: Viscosity of reference standard, Table S2: Comparison of measured density of DMEA (1) + H<sub>2</sub>O (2) mixtures with literature, Table S3: Comparison of measured viscosity of DMEA (1) + H<sub>2</sub>O (2) mixtures with literature.

**Author Contributions:** Supervision, L.E.Ø. and D.A.E.; Writing—original draft, S.S.K. All authors have read and agreed to the published version of the manuscript.

**Funding:** This work was funded by the Ministry of Education and Research of the Norwegian Government.

**Conflicts of Interest:** The authors declare no conflict of interest.

## Nomenclature

Latin Symbols		Greek Symbols	
$G_{12}$	Characteristic constant	$\eta$	Viscosity (dynamic) of the mixture, mPa·s
$\Delta G^*$	Free energy of activation for viscous flow, J·mol <sup>-1</sup>	$\eta^E$	Viscosity deviation in Equation (17), mPa·s
$\Delta G^{E*}$	Excess free energy of activation for viscous flow, J·mol <sup>-1</sup>	$\eta_i$	Viscosity of pure component, mPa·s
$h$	Planck's constant, J·s	$\eta_\gamma$	Viscosity deviation in Equation (22), mPa·s
$\Delta H^*$	Enthalpy of activation for viscous flow, J·mol <sup>-1</sup>	$\rho$	Density of the mixture, kg·m <sup>-3</sup>
$M$	Molecular weight, kg·mol <sup>-1</sup>	$\rho_i$	Density of pure components, kg·m <sup>-3</sup>
$M_1$	Molecular weight of amine, kg·mol <sup>-1</sup>	$\rho_1$	Density of pure amine, kg·m <sup>-3</sup>
$M_2$	Molecular weight of H <sub>2</sub> O, kg·mol <sup>-1</sup>	$\rho_2$	Density of pure H <sub>2</sub> O, kg·m <sup>-3</sup>
$N$	Number of data points	$\rho_\gamma$	Density deviation, kg·m <sup>-3</sup>
$N_A$	Avogadro's number, mol <sup>-1</sup>	$\nu$	Kinematic viscosity, m <sup>2</sup> ·s <sup>-1</sup>
$R$	Gas constant, J·mol <sup>-1</sup> ·K <sup>-1</sup>	$\nu_{12}, \nu_{21}$	McAllister's model parameters
$\Delta S^{E*}$	Excess entropy of activation for viscous flow, J·mol <sup>-1</sup> ·K <sup>-1</sup>		
$\Delta S^*$	Entropy of activation for viscous flow, J·mol <sup>-1</sup> ·K <sup>-1</sup>		
$T$	Temperature, K		
$V$	Molar volume of the mixture, m <sup>3</sup> ·mol <sup>-1</sup>		
$V^E$	Excess molar volume, m <sup>3</sup> ·mol <sup>-1</sup>		
$V_1^0$	Molar volume of pure amine, m <sup>3</sup> ·mol <sup>-1</sup>		
$V_2^0$	Molar volume of pure H <sub>2</sub> O, m <sup>3</sup> ·mol <sup>-1</sup>		
$\overline{V}_i$	Partial molar volume of component in the mixture, m <sup>3</sup> ·mol <sup>-1</sup>		
$\overline{V}_1$	Partial molar volume of amine in the mixture, m <sup>3</sup> ·mol <sup>-1</sup>		
$\overline{V}_2$	Partial molar volume of H <sub>2</sub> O in the mixture, m <sup>3</sup> ·mol <sup>-1</sup>		
$\overline{V}_1^\infty$	Partial molar volume of amine at infinite dilution in H <sub>2</sub> O, m <sup>3</sup> ·mol <sup>-1</sup>		
$\overline{V}_2^\infty$	Partial molar volume of H <sub>2</sub> O at infinite dilution in amine, m <sup>3</sup> ·mol <sup>-1</sup>		
$x_i$	Mole fraction of component in the mixture		
$x_1$	Mole fraction of amine in the mixture		
$x_2$	Mole fraction of H <sub>2</sub> O in the mixture		
$\gamma^E$	Excess property		
$\gamma_i^m$	Measured property		
$\gamma_i^c$	Calculated property		



Appendix A

**Table A1.** Measured density ( $\rho/\text{kg}\cdot\text{m}^{-3}$ ) and deduced excess molar volume ( $V^E/\text{m}^3\cdot\text{mol}^{-1}$ ) of MDEA (1) + H<sub>2</sub>O (2) mixtures.

T/K	<sup>a</sup> w <sub>1</sub> 0.30		0.40		0.50		0.60		0.70		0.80		0.90		0.94		0.97	
	<sup>b</sup> x <sub>1</sub> 0.0609		0.0916		0.1313		0.1849		0.2608		0.3768		0.5764		0.7031		0.8302	
	$\rho$	$10^6 \cdot V^E$	$\rho$	$10^6 \cdot V^E$	$\rho$	$10^6 \cdot V^E$	$\rho$	$10^6 \cdot V^E$	$\rho$	$10^6 \cdot V^E$	$\rho$	$10^6 \cdot V^E$	$\rho$	$10^6 \cdot V^E$	$\rho$	$10^6 \cdot V^E$	$\rho$	$10^6 \cdot V^E$
293.15	1026.9	-0.381	1036.8	-0.572	1045.6	-0.784	1052.5	-0.998	1056.5	-1.185	1056.0	-1.245	1050.7	-1.018	1046.8	-0.730	1043.7	-0.422
298.15	1024.7	-0.376	1034.2	-0.563	1042.6	-0.770	1049.2	-0.981	1052.9	-1.167	1052.4	-1.231	1047.0	-1.011	1043.2	-0.727	1040.1	-0.423
303.15	1022.4	-0.372	1031.5	-0.554	1039.5	-0.757	1045.7	-0.964	1049.3	-1.149	1048.6	-1.214	1043.3	-0.999	1039.4	-0.721	1036.3	-0.419
308.15	1019.9	-0.368	1028.6	-0.546	1036.3	-0.744	1042.2	-0.947	1045.6	-1.130	1044.9	-1.198	1039.5	-0.989	1035.7	-0.714	1032.6	-0.415
313.15	1017.3	-0.364	1025.6	-0.539	1033.0	-0.733	1038.6	-0.932	1041.8	-1.114	1041.0	-1.182	1035.7	-0.980	1031.8	-0.709	1028.8	-0.415
318.15	1014.5	-0.360	1022.5	-0.532	1029.6	-0.722	1035.0	-0.918	1038.0	-1.098	1037.1	-1.166	1031.8	-0.969	1028.0	-0.702	1024.9	-0.411
323.15	1011.7	-0.357	1019.4	-0.525	1026.1	-0.711	1031.2	-0.903	1034.1	-1.080	1033.2	-1.150	1027.9	-0.958	1024.1	-0.695	1021.1	-0.404
328.15	1008.7	-0.354	1016.1	-0.519	1022.5	-0.701	1027.4	-0.889	1030.2	-1.064	1029.2	-1.133	1024.0	-0.946	1020.2	-0.686	1017.2	-0.400
333.15	1005.5	-0.349	1012.7	-0.512	1018.9	-0.691	1023.6	-0.875	1026.2	-1.047	1025.1	-1.116	1020.0	-0.934	1016.3	-0.679	1013.3	-0.396
338.15	1002.2	-0.345	1009.2	-0.505	1015.1	-0.680	1019.6	-0.861	1022.1	-1.030	1021.0	-1.098	1015.8	-0.912	1012.3	-0.668	1009.4	-0.393
343.15	998.6	-0.335	1005.4	-0.492	1011.3	-0.670	1015.6	-0.847	1018.0	-1.013	1016.9	-1.080	1011.9	-0.909	1008.3	-0.659	1005.5	-0.388
348.15			1001.5	-0.481	1007.4	-0.659	1011.5	-0.832	1013.8	-0.995	1012.7	-1.062	1007.8	-0.895	1004.3	-0.649	1001.5	-0.383
353.15			996.9	-0.450	1003.4	-0.646	1007.3	-0.813	1009.5	-0.977	1008.4	-1.042	1003.7	-0.879	1000.3	-0.636	997.5	-0.375

<sup>a</sup> mass fraction, <sup>b</sup> mole fraction of MDEA.

**Table A2.** Measured density ( $\rho/\text{kg}\cdot\text{m}^{-3}$ ) and deduced excess molar volume ( $V^E/\text{m}^3\cdot\text{mol}^{-1}$ ) of DMEA (1) + H<sub>2</sub>O (2) mixtures.

T/K	<sup>a</sup> w <sub>1</sub> 0.30		0.40		0.50		0.60		0.70		0.80		0.90		0.94		0.97	
	<sup>b</sup> x <sub>1</sub> 0.0797		0.1187		0.1681		0.2326		0.3204		0.4470		0.6452		0.7600		0.8673	
	$\rho$	$10^6 \cdot V^E$	$\rho$	$10^6 \cdot V^E$	$\rho$	$10^6 \cdot V^E$	$\rho$	$10^6 \cdot V^E$	$\rho$	$10^6 \cdot V^E$	$\rho$	$10^6 \cdot V^E$	$\rho$	$10^6 \cdot V^E$	$\rho$	$10^6 \cdot V^E$	$\rho$	$10^6 \cdot V^E$
293.15	991.0	-0.712	987.1	-1.020	979.9	-1.305	969.3	-1.550	954.9	-1.704	936.6	-1.678	914.2	-1.274	904.2	-0.931	896.5	-0.567
298.15	988.2	-0.704	983.8	-1.004	976.2	-1.286	965.4	-1.534	950.9	-1.692	932.6	-1.675	910.1	-1.279	900.2	-0.941	892.4	-0.579
303.15	985.4	-0.696	980.3	-0.990	972.3	-1.268	961.4	-1.518	946.8	-1.680	928.4	-1.668	906.0	-1.284	896.0	-0.947	888.3	-0.589
308.15	982.4	-0.689	976.8	-0.977	968.4	-1.253	957.3	-1.502	942.7	-1.669	924.3	-1.666	901.8	-1.287	891.8	-0.956	884.0	-0.591
313.15	979.2	-0.683	973.1	-0.965	964.5	-1.239	953.2	-1.488	938.4	-1.659	920.0	-1.661	897.5	-1.291	887.6	-0.960	879.7	-0.596
318.15	976.0	-0.679	969.5	-0.957	960.5	-1.226	949.0	-1.476	934.1	-1.649	915.7	-1.657	893.3	-1.295	883.3	-0.964	875.4	-0.601
323.15	972.7	-0.674	965.7	-0.948	956.4	-1.215	944.7	-1.464	929.8	-1.640	911.3	-1.653	888.9	-1.298	878.9	-0.968	871.0	-0.603
328.15	969.3	-0.670	961.9	-0.941	952.3	-1.205	940.4	-1.454	925.4	-1.632	906.9	-1.649	884.5	-1.301	874.5	-0.973	866.6	-0.605
333.15	965.8	-0.668	958.0	-0.934	948.1	-1.195	936.0	-1.444	920.9	-1.624	902.4	-1.645	880.0	-1.301	870.0	-0.973	862.2	-0.611
338.15	962.1	-0.665	954.0	-0.928	943.8	-1.187	931.5	-1.435	916.4	-1.616	897.9	-1.643	875.5	-1.304	865.6	-0.980	857.6	-0.613
343.15	958.3	-0.663	950.0	-0.928	939.5	-1.184	927.0	-1.433	911.8	-1.617	893.2	-1.650	870.9	-1.322	861.0	-1.007	853.1	-0.642
348.15	954.3	-0.652	945.7	-0.914	935.1	-1.170	922.4	-1.414	907.1	-1.596	888.6	-1.625	866.3	-1.292	856.4	-0.973	848.5	-0.604
353.15	950.4	-0.653	941.5	-0.912	930.7	-1.172	917.8	-1.413	902.3	-1.596	882.5	-1.546	861.6	-1.306	851.7	-0.989	843.9	-0.633

<sup>a</sup> mass fraction, <sup>b</sup> mole fraction of DMEA.

**Table A3.** Measured density ( $\rho/\text{kg}\cdot\text{m}^{-3}$ ) and deduced excess molar volume ( $V^E/\text{m}^3\cdot\text{mol}^{-1}$ ) of DEEA (1) + H<sub>2</sub>O (2) mixtures.

T/K	<sup>a</sup> w <sub>1</sub> 0.30		0.40		0.50		0.60		0.70		0.80		0.90		0.94		0.97	
	<sup>b</sup> x <sub>1</sub> 0.0618		0.0930		0.1332		0.1874		0.2640		0.3808		0.5805		0.7066		0.8325	
	$\rho$	$10^6 \cdot V^E$	$\rho$	$10^6 \cdot V^E$	$\rho$	$10^6 \cdot V^E$	$\rho$	$10^6 \cdot V^E$	$\rho$	$10^6 \cdot V^E$	$\rho$	$10^6 \cdot V^E$	$\rho$	$10^6 \cdot V^E$	$\rho$	$10^6 \cdot V^E$	$\rho$	$10^6 \cdot V^E$
293.15	989.6	-0.724	983.2	-0.990	974.6	-1.258	963.9	-1.531	950.8	-1.786	934.4	-1.941	912.9	-1.706	902.4	-1.313	893.6	-0.788
298.15	986.6	-0.712	979.7	-0.973	970.7	-1.240	959.8	-1.513	946.5	-1.771	930.0	-1.932	908.5	-1.707	897.9	-1.319	889.1	-0.800
303.15	983.4	-0.701	976.0	-0.957	966.7	-1.222	955.6	-1.497	942.0	-1.755	925.4	-1.922	903.9	-1.705	893.3	-1.321	884.5	-0.802
308.15	980.2	-0.692	972.3	-0.944	962.6	-1.206	951.2	-1.481	937.6	-1.742	920.8	-1.913	899.2	-1.695	888.7	-1.327	879.9	-0.808
313.15	976.8	-0.684	968.5	-0.931	958.5	-1.191	946.8	-1.465	933.0	-1.727	916.1	-1.898	894.6	-1.699	884.0	-1.324	875.2	-0.809
318.15	973.4	-0.676	964.6	-0.920	954.3	-1.177	942.4	-1.450	928.4	-1.712	911.4	-1.888	889.8	-1.693	879.3	-1.324	870.5	-0.812
323.15	969.8	-0.669	960.6	-0.909	950.0	-1.164	937.8	-1.436	923.6	-1.698	906.6	-1.875	884.9	-1.677	874.5	-1.322	865.7	-0.809
328.15	966.2	-0.663	956.5	-0.900	945.6	-1.152	933.2	-1.422	918.8	-1.683	901.7	-1.861	880.2	-1.679	869.7	-1.316	861.0	-0.807
333.15	962.4	-0.657	952.4	-0.890	941.1	-1.140	928.5	-1.407	914.0	-1.666	896.8	-1.850	875.3	-1.668	864.8	-1.308	856.1	-0.804
338.15	958.5	-0.651	948.2	-0.881	936.6	-1.127	923.8	-1.393	909.1	-1.650	891.7	-1.822	870.3	-1.655	859.9	-1.294	851.3	-0.804
343.15	954.6	-0.645	943.8	-0.872	932.0	-1.115	919.0	-1.379	904.1	-1.633	886.6	-1.806	865.3	-1.639	854.9	-1.282	846.4	-0.799
348.15	950.5	-0.641	939.5	-0.863	927.3	-1.102	914.1	-1.363	899.1	-1.617	881.5	-1.786	860.2	-1.621	849.9	-1.270	841.4	-0.788
353.15	946.3	-0.632	935.0	-0.853	922.6	-1.091	909.1	-1.346	893.8	-1.592	876.3	-1.763	855.0	-1.599	844.8	-1.252	836.4	-0.776

<sup>a</sup> mass fraction, <sup>b</sup> mole fraction of DEEA.

**Table A4.** Partial molar volume  $\overline{V}_1^\infty/\text{m}^3\cdot\text{mol}^{-1}$  of MDEA, DMEA, and DEEA at infinite dilution in H<sub>2</sub>O and molar volume of pure species  $V_1^0/\text{m}^3\cdot\text{mol}^{-1}$  at various temperatures.

T/K	MDEA (1) at Infinite Dilution in H <sub>2</sub> O (2)			DMEA (1) at Infinite Dilution in H <sub>2</sub> O (2)			DEEA (1) at Infinite Dilution in H <sub>2</sub> O (2)		
	$10^6 \cdot \overline{V}_1^\infty$	$10^6 \cdot \overline{V}_1^\infty$ Literature	$10^6 \cdot V_1^0$	$10^6 \cdot \overline{V}_1^\infty$	$10^6 \cdot \overline{V}_1^\infty$ Literature	$10^6 \cdot V_1^0$	$10^6 \cdot \overline{V}_1^\infty$	$10^6 \cdot \overline{V}_1^\infty$ Literature	$10^6 \cdot V_1^0$
293.15	108.7		114.5	92.0	93.6 <sup>c,d</sup>	100.4	118.9	122.1 <sup>d,e</sup>	132.5
298.15	109.1	109.5 <sup>a</sup> , 108.9 <sup>b</sup>	114.9	92.4	93.7 <sup>b</sup> , 94.1 <sup>c</sup> , 93.9 <sup>c,d</sup>	100.9	119.6	117.6 <sup>b</sup> , 122.6 <sup>e</sup> , 122.7 <sup>d,e</sup>	133.2
303.15	109.6	110.7 <sup>a</sup>	115.3	92.8	94.3 <sup>c</sup> , 94.2 <sup>c,d</sup>	101.4	120.4	123.0 <sup>e</sup> , 122.7 <sup>d,e</sup>	133.9
308.15	110.0	110.0 <sup>b</sup>	115.8	93.3	95.7 <sup>b</sup>	101.9	121.2	118.0 <sup>b</sup>	134.6
313.15	110.5	110.7 <sup>a</sup>	116.2	93.7	94.8 <sup>c</sup> , 94.9 <sup>c,d</sup>	102.4	122.0	123.7 <sup>e</sup> , 123.6 <sup>d,e</sup>	135.4
318.15	110.9	110.7 <sup>b</sup>	116.6	94.2	97.2 <sup>b</sup>	102.9	122.8	118.3 <sup>b</sup>	136.1
323.15	111.4	111.4 <sup>a</sup>	117.1	94.6		103.4	123.6		136.9
328.15	111.8		117.5	95.1		103.9	124.4		137.6
333.15	112.3	112.5 <sup>a</sup>	118.0	95.6	96.3 <sup>c</sup>	104.5	125.2	125.3 <sup>e</sup>	138.4
338.15	112.8		118.4	96.1		105.0	126.1		139.2
343.15	113.3	113.1 <sup>a</sup>	118.9	96.6		105.6	126.9		140.0
348.15	113.7		119.3	97.1		106.2	127.8		140.8
353.15	114.2	113.8 <sup>a</sup>	119.8	97.6	98.1 <sup>c</sup>	106.8	128.7	128.0 <sup>e</sup>	141.6

Literature references: <sup>a</sup> Maham et al. [17], <sup>b</sup> Hawrylak et al. [16], <sup>c</sup> Maham et al. [18], <sup>d</sup> Zhang et al. [19], <sup>e</sup> Lebrette et al. [20].

**Table A5.** Measured viscosity ( $\eta$ /mPa·s) and deduced viscosity deviation ( $\eta^E$ /mPa·s) of MDEA (1) + H<sub>2</sub>O (2) mixtures.

T/K	<sup>a</sup> w <sub>1</sub> 0.30		0.40		0.50		0.60		0.70		0.80		0.90		0.94		0.97	
	<sup>b</sup> x <sub>1</sub> 0.0609		0.0916		0.1313		0.1849		0.2608		0.3768		0.5764		0.7031		0.8302	
	$\eta$	$\eta^E$	$\eta$	$\eta^E$	$\eta$	$\eta^E$	$\eta$	$\eta^E$	$\eta$	$\eta^E$	$\eta$	$\eta^E$	$\eta$	$\eta^E$	$\eta$	$\eta^E$	$\eta$	$\eta^E$
293.15	3.712	-3.358	6.410	-3.723	11.633	-2.465	21.915	2.480	42.784	15.778	76.266	37.686	107.892	49.414	111.511	40.394	108.675	24.890
298.15	3.136	-2.319	5.290	-2.468	9.323	-1.418	16.721	1.965	32.161	11.711	56.123	26.967	79.249	35.126	82.357	28.727	80.921	17.762
303.15	2.673	-1.594	4.410	-1.609	7.561	-0.725	13.075	1.737	24.522	8.854	41.834	19.548	58.937	25.273	61.546	20.654	60.950	12.815
308.15	2.301	-1.090	3.721	-1.018	6.200	-0.285	10.404	1.570	18.988	6.821	31.721	14.458	44.492	18.469	46.689	15.102	46.555	9.390
313.15	1.995	-0.742	3.170	-0.618	5.152	0.002	8.418	1.435	14.936	5.354	24.435	10.879	34.108	13.719	35.949	11.220	36.084	7.005
318.15	1.748	-0.496	2.732	-0.343	4.335	0.183	6.916	1.315	11.930	4.273	19.137	8.338	26.566	10.363	28.108	8.473	28.378	5.304
323.15	1.544	-0.322	2.376	-0.155	3.683	0.289	5.759	1.205	9.659	3.460	15.206	6.490	20.977	7.936	22.277	6.489	22.607	4.065
328.15	1.376	-0.199	2.088	-0.027	3.168	0.353	4.863	1.106	7.938	2.846	12.272	5.138	16.823	6.179	17.927	5.053	18.264	3.155
333.15	1.236	-0.109	1.849	0.062	2.749	0.389	4.147	1.014	6.600	2.372	10.019	4.117	13.644	4.865	14.580	3.973	14.924	2.485
338.15	1.117	-0.043	1.649	0.121	2.408	0.406	3.572	0.930	5.554	2.005	8.281	3.346	11.201	3.882	11.996	3.163	12.326	1.975
343.15	1.017	0.006	1.478	0.161	2.128	0.414	3.104	0.856	4.722	1.716	6.923	2.760	9.291	3.136	9.962	2.543	10.278	1.591
348.15	0.930	0.041	1.335	0.188	1.894	0.413	2.723	0.792	4.055	1.486	5.844	2.300	7.788	2.567	8.353	2.067	8.642	1.289
353.15	0.853	0.066	1.213	0.206	1.698	0.408	2.407	0.736	3.513	1.301	4.984	1.943	6.587	2.124	7.065	1.698	7.337	1.064
358.15	0.790	0.086	1.108	0.218	1.528	0.394	2.144	0.685	3.072	1.149	4.290	1.659	5.619	1.772	6.026	1.406	6.268	0.873
363.15	0.747	0.114	1.018	0.224	1.377	0.374	1.925	0.641	2.710	1.028	3.725	1.434	4.834	1.494	5.181	1.1761	5.395	0.723

<sup>a</sup> mass fraction, <sup>b</sup> mole fraction of MDEA.

**Table A6.** Measured viscosity ( $\eta$ /mPa·s) and deduced viscosity deviation ( $\eta^E$ /mPa·s) of DMEA (1) + H<sub>2</sub>O (2) mixtures.

T/K	<sup>a</sup> w <sub>1</sub> 0.30		0.40		0.50		0.60		0.70		0.80		0.90		0.94		0.97	
	<sup>b</sup> x <sub>1</sub> 0.0797		0.1187		0.1681		0.2326		0.3204		0.4470		0.6452		0.7600		0.8673	
	$\eta$	$\eta^E$	$\eta$	$\eta^E$	$\eta$	$\eta^E$	$\eta$	$\eta^E$	$\eta$	$\eta^E$	$\eta$	$\eta^E$	$\eta$	$\eta^E$	$\eta$	$\eta^E$	$\eta$	$\eta^E$
293.15	4.214	2.981	6.814	5.469	10.169	8.681	14.010	12.335	16.750	14.822	15.539	13.245	9.712	6.845	7.129	3.931	5.383	1.875
298.15	3.457	2.367	5.464	4.278	8.011	6.701	10.886	9.416	12.989	11.299	12.214	10.208	7.955	5.454	5.976	3.189	4.591	1.537
303.15	2.869	1.900	4.446	3.392	6.398	5.237	8.571	7.271	10.197	8.707	9.704	7.941	6.565	4.374	5.031	2.593	3.937	1.267
308.15	2.413	1.545	3.664	2.723	5.189	4.155	6.848	5.694	8.120	6.802	7.796	6.241	5.458	3.533	4.264	2.124	3.391	1.052
313.15	2.055	1.272	3.060	2.215	4.262	3.336	5.548	4.517	6.540	5.366	6.340	4.961	4.577	2.877	3.637	1.750	2.937	0.876
318.15	1.768	1.059	2.590	1.825	3.552	2.718	4.562	3.636	5.362	4.312	5.220	3.990	3.877	2.367	3.131	1.459	2.564	0.740
323.15	1.536	0.890	2.216	1.521	2.999	2.244	3.794	2.958	4.442	3.497	4.340	3.239	3.307	1.959	2.708	1.218	2.249	0.625
328.15	1.349	0.757	1.918	1.284	2.564	1.876	3.199	2.441	3.723	2.868	3.652	2.659	2.845	1.635	2.363	1.028	1.987	0.535
333.15	1.193	0.649	1.676	1.094	2.215	1.586	2.725	2.034	3.151	2.375	3.099	2.200	2.462	1.371	2.071	0.870	1.765	0.460
338.15	1.064	0.562	1.478	0.943	1.934	1.356	2.346	1.712	2.703	1.994	2.653	1.835	2.146	1.158	1.828	0.741	1.575	0.397
343.15	0.955	0.490	1.315	0.821	1.701	1.169	2.038	1.457	2.324	1.676	2.289	1.544	1.882	0.985	1.621	0.637	1.413	0.347
348.15	0.865	0.434	1.179	0.721	1.505	1.014	1.786	1.251	2.022	1.428	1.988	1.308	1.658	0.844	1.444	0.552	1.274	0.309

**Table A6.** *Cont.*

T/K	<sup>a</sup> w <sub>1</sub>		0.30		0.40		0.50		0.60		0.70		0.80		0.90		0.94		0.97	
	<sup>b</sup> x <sub>1</sub>		0.0797		0.1187		0.1681		0.2326		0.3204		0.4470		0.6452		0.7600		0.8673	
	η	η <sup>E</sup>	η	η <sup>E</sup>	η	η <sup>E</sup>	η	η <sup>E</sup>	η	η <sup>E</sup>	η	η <sup>E</sup>	η	η <sup>E</sup>	η	η <sup>E</sup>	η	η <sup>E</sup>	η	η <sup>E</sup>
353.15	0.790	0.388	1.064	0.638	1.341	0.886	1.572	1.078	1.770	1.223	1.739	1.115	1.468	0.725	1.291	0.478	1.151	0.274		
358.15	0.722	0.347	0.968	0.571	1.203	0.780	1.401	0.943	1.560	1.055	1.532	0.958	1.308	0.626	1.159	0.416	1.045	0.244		
363.15	0.674	0.323	0.884	0.514	1.080	0.686	1.251	0.826	1.385	0.917	1.358	0.829	1.170	0.544	1.046	0.365	0.954	0.221		

<sup>a</sup> mass fraction, <sup>b</sup> mole fraction of DMEA.

**Table A7.** Measured viscosity (η/mPa·s) and deduced viscosity deviation (η<sup>E</sup>/mPa·s) of DEEA (1) + H<sub>2</sub>O (2) mixtures.

T/K	<sup>a</sup> w <sub>1</sub>		0.30		0.40		0.50		0.60		0.70		0.80		0.90		0.94		0.97	
	<sup>b</sup> x <sub>1</sub>		0.0618		0.0930		0.1332		0.1874		0.2640		0.3808		0.5805		0.7066		0.8325	
	η	η <sup>E</sup>	η	η <sup>E</sup>	η	η <sup>E</sup>	η	η <sup>E</sup>	η	η <sup>E</sup>	η	η <sup>E</sup>	η	η <sup>E</sup>	η	η <sup>E</sup>	η	η <sup>E</sup>	η	η <sup>E</sup>
293.15	4.511	3.266	7.057	5.688	10.454	8.927	14.648	12.907	18.849	16.806	20.569	18.064	15.023	11.730	10.786	6.996	7.593	3.305		
298.15	3.666	2.573	5.616	4.421	8.157	6.829	11.239	9.734	14.255	12.499	15.446		11.561	8.767	8.548	5.340	6.191	2.570		
303.15	3.025	2.059	4.536	3.484	6.477	5.315	8.731	7.420	10.922	9.401	11.757	13.307	9.009	6.623	6.905	4.173	5.092	2.016		
308.15	2.529	1.668	3.713	2.781	5.222	4.197	6.903	5.755	8.510	7.185	9.104	9.917	7.122	5.072	5.607	3.268	4.223	1.595		
313.15	2.143	1.371	3.090	2.257	4.223	3.312	5.546	4.531	6.740	5.577	7.161	7.512	5.711	3.938	4.609	2.592	3.536	1.276		
318.15	1.839	1.141	2.607	1.858	3.517	2.702	4.533	3.629	5.425	4.396	5.729	5.774	4.649	3.101	3.810	2.055	2.999	1.038		
323.15	1.597	0.964	2.226	1.549	2.964	2.230	3.750	2.940	4.432	3.514	4.650	4.509	3.822	2.461	3.184	1.646	2.560	0.845		
328.15	1.397	0.819	1.926	1.309	2.535	1.869	3.151	2.420	3.676	2.852	3.832	3.569	3.187	1.981	2.704	1.346	2.205	0.695		
333.15	1.238	0.707	1.678	1.115	2.189	1.583	2.675	2.013	3.086	2.343	3.196	2.867	2.697	1.624	2.302	1.097	1.919	0.582		
338.15	1.105	0.616	1.480	0.962	1.911	1.356	2.311	1.707	2.619	1.944	2.703	2.332	2.282	1.319	1.981	0.902	1.678	0.485		
343.15	0.998	0.545	1.314	0.836	1.682	1.171	2.010	1.456	2.265	1.649	2.304	1.922	1.967	1.097	1.717	0.746	1.477	0.405		
348.15	0.905	0.484	1.180	0.736	1.491	1.018	1.756	1.245	1.943	1.378	1.983	1.594	1.681	0.891	1.513	0.633	1.310	0.341		
353.15	0.834	0.441	1.076	0.663	1.330	0.892	1.545	1.073	1.697	1.177	1.717	1.335	1.471	0.751	1.342	0.542	1.172	0.293		
358.15	0.765	0.398	0.984	0.599	1.194	0.786	1.372	0.934	1.493	1.012	1.497	1.123	1.299	0.640	1.183	0.452	1.059	0.257		
363.15	0.703	0.359	0.906	0.546	1.077	0.697	1.221	0.814	1.316	0.871	1.321	0.950	1.154	0.549	1.052	0.384	0.961	0.230		

<sup>a</sup> mass fraction, <sup>b</sup> mole fraction of DEEA.

## References

1. Metz, B.; Davidson, O.; Coninck, H.D.; Loos, M.; Meyer, L. IPCC Special Report on Carbon Dioxide Capture and Storage. Cambridge University Press: New York, NY, USA, 2005.
2. Nwaoha, C.; Tontiwachwuthikul, P.; Benamor, A. A comparative study of novel activated AMP using 1,5-diamino-2-methylpentane vs MEA solution for CO<sub>2</sub> capture from gas-fired power plant. *Fuel* **2018**, *234*, 1089–1098. [[CrossRef](#)]
3. Nwaoha, C.; Saiwan, C.; Supap, T.; Idem, R.; Tontiwachwuthikul, P.; Rongwong, W.; Al-Marri, M.J.; Benamor, A. Carbon dioxide (CO<sub>2</sub>) capture performance of aqueous tri-solvent blends containing 2-amino-2-methyl-1-propanol (AMP) and methyldiethanolamine (MDEA) promoted by diethylenetriamine (DETA). *Int. J. Greenh. Gas Control* **2016**, *53*, 292–304. [[CrossRef](#)]
4. Kim, C.J.; Savage, D.W. Kinetics of carbon dioxide reaction with diethylaminoethanol in aqueous solutions. *Chem. Eng. Sci.* **1987**, *42*, 1481–1487. [[CrossRef](#)]
5. Rinker, E.B.; Sami, S.A.; Sandall, O.C. Kinetics and modelling of carbon dioxide absorption into aqueous solutions of N-methyldiethanolamine. *Chem. Eng. Sci.* **1995**, *50*, 755–768. [[CrossRef](#)]
6. Monteiro, J.G.M.S.; Pinto, D.D.D.; Zaidy, S.A.H.; Hartono, A.; Svendsen, H.F. VLE data and modelling of aqueous N,N-diethylethanolamine (DEEA) solutions. *Int. J. Greenh. Gas Control* **2013**, *19*, 432–440. [[CrossRef](#)]
7. Henni, A.; Li, J.; Tontiwachwuthikul, P. Reaction kinetics of CO<sub>2</sub> in aqueous 1-Amino-2-Propanol, 3-Amino-1-Propanol, and Dimethylmonoethanolamine solutions in the temperature range of 298–313 K using the stopped-flow technique. *Ind. Eng. Chem. Res.* **2008**, *47*, 2213–2220. [[CrossRef](#)]
8. Zhang, J.; Fennell, P.S.; Trusler, J.P.M. Density and viscosity of partially carbonated aqueous tertiary Alkanolamine solutions at temperatures between (298.15 and 353.15) K. *J. Chem. Eng. Data* **2015**, *60*, 2392–2399. [[CrossRef](#)]
9. Versteeg, G.F.; Van Swaaij, W.P.M. Solubility and diffusivity of acid gases (carbon dioxide, nitrous oxide) in aqueous alkanolamine solutions. *J. Chem. Eng. Data* **1988**, *33*, 29–34. [[CrossRef](#)]
10. Aronu, U.E.; Hartono, A.; Svendsen, H.F. Density, viscosity, and N<sub>2</sub>O solubility of aqueous amino acid salt and amine amino acid salt solutions. *J. Chem. Thermodyn.* **2012**, *45*, 90–99. [[CrossRef](#)]
11. Cleeton, C.; Kvam, O.; Rea, R.; Sarkisov, L.; De Angelis, M.G. Competitive H<sub>2</sub>S – CO<sub>2</sub> absorption in reactive aqueous methyldiethanolamine solution: Prediction with ePC-SAFT. *Fluid Phase Equilib.* **2020**, *511*, 112453. [[CrossRef](#)]
12. Wangler, A.; Sieder, G.; Ingram, T.; Heilig, M.; Held, C. Prediction of CO<sub>2</sub> and H<sub>2</sub>S solubility and enthalpy of absorption in reacting N-methyldiethanolamine/water systems with ePC-SAFT. *Fluid Phase Equilib.* **2018**, *461*, 15–27. [[CrossRef](#)]
13. Idris, Z.; Kummamuru, N.B.; Eimer, D.A. Viscosity measurement of unloaded and CO<sub>2</sub>-loaded aqueous monoethanolamine at higher concentrations. *J. Mol. Liq.* **2017**, *243*, 638–645. [[CrossRef](#)]
14. JCGM. Evaluation of Measurement Data—Supplement 1 to the “Guide to the Expression of Uncertainty in Measurement”—Propagation of Distributions Using a Monte Carlo Method. Available online: [https://www.bipm.org/utis/common/documents/jcgm/JCGM\\_101\\_2008\\_E.pdf](https://www.bipm.org/utis/common/documents/jcgm/JCGM_101_2008_E.pdf) (accessed on 3 January 2020).
15. Ellison, S.L.R.; Williams, A. Quantifying Uncertainty in Analytical Measurement. Available online: [https://www.eurachem.org/images/stories/Guides/pdf/QUAM2012\\_P1.pdf](https://www.eurachem.org/images/stories/Guides/pdf/QUAM2012_P1.pdf) (accessed on 3 January 2020).
16. Hawrylak, B.; Bruke, S.E.; Palepu, R. Partial molar and excess volumes and adiabatic compressibilities of binary mixtures of ethanolamines with water. *J. Solut. Chem.* **2000**, *29*, 575–593. [[CrossRef](#)]
17. Maham, Y.; Teng, T.T.; Mather, A.E.; Hepler, L.G. Volumetric properties of (water + diethanolamine) systems. *Can. J. Chem.* **1995**, *73*, 1514–1519. [[CrossRef](#)]
18. Maham, Y.; Teng, T.T.; Hepler, L.G.; Mather, A.E. Volumetric properties of aqueous solutions of monoethanolamine, mono- and dimethylethanolamines at temperatures from 5 to 80 °C I. *Thermochim. Acta* **2002**, *386*, 111–118. [[CrossRef](#)]
19. Zhang, F.-Q.; Li, H.-P.; Dai, M.; Zhao, J.-P.; Chao, J.P. Volumetric properties of binary mixtures of water with ethanolamine alkyl derivatives. *Thermochim. Acta* **1995**, *254*, 347–357. [[CrossRef](#)]
20. Lebrette, L.; Maham, Y.; Teng, T.T.; Hepler, L.G.; Mather, A.E. Volumetric properties of aqueous solutions of mono, and diethylethanolamines at temperatures from 5 to 80 °C II. *Thermochim. Acta* **2002**, *386*, 119–126. [[CrossRef](#)]

21. Concepción, E.I.; Gómez-Hernández, Á.; Martín, M.C.; Segovia, J.J. Density and viscosity measurements of aqueous amines at high pressures: DEA-water, DMAE-water and TEA-water mixtures. *J. Chem. Thermodyn.* **2017**, *112*, 227–239. [[CrossRef](#)]
22. Ma, D.; Liu, Q.; Zhu, C.; Feng, H.; Ma, Y. Volumetric and viscometric properties of ternary solution of (N-methyldiethanolamine + monoethanolamine + ethanol). *J. Chem. Thermodyn.* **2019**, *134*, 5–19. [[CrossRef](#)]
23. Begum, S.K.; Clarke, R.J.; Ahmed, M.S.; Begum, S.; Saleh, M.A. Volumetric, viscosimetric and surface properties of aqueous solutions of triethylene glycol, tetraethylene glycol, and tetraethylene glycol dimethyl ether. *J. Mol. Liq.* **2013**, *177*, 11–18. [[CrossRef](#)]
24. Rafiee, H.R.; Frouzesh, F. Volumetric properties for binary and ternary mixtures of allyl alcohol, 1,3-dichloro-2-propanol and 1-ethyl-3-methyl imidazolium ethyl sulfate [Emim][EtSO<sub>4</sub>] from T=298.15 to 318.15K at ambient pressure. *Thermochim. Acta* **2015**, *611*, 36–46. [[CrossRef](#)]
25. Aminabhavi, T.M.; Aralaguppi, M.I.; Bindu, G.; Khinnavar, R.S. Densities, shear viscosities, refractive indices, and speeds of sound of Bis(2-methoxyethyl) Ether with Hexane, Heptane, Octane, and 2,2,4-Trimethylpentane in the temperature interval 298.15-318.15 K. *J. Chem. Eng. Data* **1994**, *39*, 522–528. [[CrossRef](#)]
26. Harvey, A.H. *Thermodynamic Properties of Water*; NIST: Boulder, CO, USA, 1998.
27. Hartono, A.; Svendsen, H.F. Density, viscosity, and excess properties of aqueous solution of diethylenetriamine (DETA). *J. Chem. Thermodyn.* **2009**, *41*, 973–979. [[CrossRef](#)]
28. Redlich, O.; Kister, A.T. Algebraic representation of thermodynamic properties and the classification of solutions. *Ind. Eng. Chem.* **1948**, *40*, 345–348. [[CrossRef](#)]
29. Maham, Y.; Teng, T.T.; Hepler, L.G.; Mather, A.E. Densities, excess molar volumes, and partial molar volumes for binary mixtures of Water with Monoethanolamine, Diethanolamine, and Triethanolamine from 25 to 80 °C. *J. Solut. Chem.* **1994**, *23*, 195–205. [[CrossRef](#)]
30. Hepler, L.G. Thermal expansion and structure in water and aqueous solutions. *Can. J. Chem.* **1969**, *47*, 4613–4617. [[CrossRef](#)]
31. Teng, T.T.; Maham, Y.; Hepler, L.G.; Mather, A.E. Viscosity of aqueous solutions of N-Methyldiethanolamine and of Diethanolamine. *J. Chem. Eng. Data* **1994**, *39*, 290–293. [[CrossRef](#)]
32. Bernal-García, J.M.; Hall, K.R.; Estrada-Baltazar, A.; Iglesias-Silva, G.A. Density and viscosity of aqueous solutions of N,N-dimethylethanolamine at p = 0.1 MPa from T=(293.15 to 363.15) K. *J. Chem. Thermodyn.* **2005**, *37*, 762–767. [[CrossRef](#)]
33. Maham, Y.; Lebrette, L.; Mather, A.E. Viscosities and excess properties of aqueous solutions of Mono- and Diethylethanolamines at temperatures between 298.15 and 353.15 K. *J. Chem. Eng. Data* **2002**, *47*, 550–553. [[CrossRef](#)]
34. Korson, L.; Hansen, W.D.; Millero, F.J. Viscosity of water at various temperatures. *J. Phys. Chem.* **1969**, *73*, 34–39. [[CrossRef](#)]
35. Kauzmann, W.; Eyring, H. The viscous flow of large molecules. *J. Am. Chem. Soc.* **1940**, *62*, 3113–3125. [[CrossRef](#)]
36. Oskoei, A.G.; Safaei, N.; Ghasemi, J. Densities and viscosities for binary and ternary mixtures of 1, 4-Dioxane + 1-Hexanol + N,N-Dimethylaniline from T = (283.15 to 343.15) K. *J. Chem. Eng. Data* **2008**, *53*, 343–349. [[CrossRef](#)]
37. Fort, R.J.; Moore, W.R. Viscosities of binary liquid mixtures. *Trans. Faraday Soc.* **1966**, *62*, 1112–1119. [[CrossRef](#)]
38. Bhatia, S.C.; Bhatia, R.; Dubey, G.P. Studies on transport and thermodynamic properties of binary mixtures of octan-1-ol with chloroform, 1,2-dichloroethane and 1,1,2,2-tetrachloroethane at 298.15 and 308.15 K. *J. Mol. Liq.* **2009**, *144*, 163–171. [[CrossRef](#)]
39. Grunberg, L.; Nissan, A.H. Mixture law for viscosity. *Nature* **1949**, *164*, 799–800. [[CrossRef](#)]
40. Eyring, H. Viscosity, Plasticity, and Diffusion as example of absolute reaction rates. *J. Chem. Phys.* **1936**, *4*, 283–291. [[CrossRef](#)]
41. Meyer, R.; Meyer, M.; Metzger, J.; Peneloux, A. Thermodynamic and physicochemical properties of binary solvent. *J. Chim. Phys. Phys. Chim. Biol.* **1971**, *68*, 406–412. [[CrossRef](#)]
42. Kinart, C.M.; Kinart, W.J.; Ćwiklińska, A. 2-Methoxyethanol–Tetrahydrofuran–binary liquid system. Viscosities, densities, excess molar volumes and excess Gibbs activation energies of viscous flow at various temperatures. *J. Therm. Anal. Calorim.* **2002**, *68*, 307–317. [[CrossRef](#)]

43. Oswal, S.; Rathnam, M.V. Viscosity data of binary mixtures: Ethyl acetate + cyclohexane, + benzene, + toluene, + ethylbenzene + carbon tetrachloride, and + chloroform at 303.15 K. *Can. J. Chem.* **1984**, *62*, 2851–2853. [[CrossRef](#)]
44. Ćwiklińska, A.; Kinart, C.M. Thermodynamic and physicochemical properties of binary mixtures of nitromethane with {2-methoxyethanol+2-butoxyethanol} systems at T= (293.15, 298.15, 303.15, 308.15, and 313.15)K. *J. Chem. Thermodyn.* **2011**, *43*, 420–429. [[CrossRef](#)]
45. Hartono, A.; Mba, E.O.; Svendsen, H.F. Physical properties of partially CO<sub>2</sub> loaded aqueous monoethanolamine (MEA). *J. Chem. Eng. Data* **2014**, *59*, 1808–1816. [[CrossRef](#)]
46. McAllister, R.A. The viscosity of liquid mixtures. *AIChE J.* **1960**, *6*, 427–431. [[CrossRef](#)]
47. Karunarathne, S.S.; Øi, L.E. Density and viscosity correlations for aqueous 3-amino-1-propanol and monoethanol amine mixtures. Proceedings of SIMS 60, Västerås, Sweden, 13–16 August 2019.



© 2020 by the authors. Licensee MDPI, Basel, Switzerland. This article is an open access article distributed under the terms and conditions of the Creative Commons Attribution (CC BY) license (<http://creativecommons.org/licenses/by/4.0/>).